Linking Switzerland's PM_{10} and $PM_{2.5}$ oxidative potential (OP) with emission sources

Stuart K. Grange[1,2], Gaëlle Uzu[3], Samuël Weber[3], Jean-Luc Jaffrezo[3], and Christoph Hueglin[1]

[1]Empa, Swiss Federal Laboratories for Materials Science and Technology, Überlandstrasse 129, 8600 Dübendorf, Switzerland
[2]Wolfson Atmospheric Chemistry Laboratories, University of York, York, YO10 5DD, United Kingdom
[3]Université Grenoble Alpes, IRD, CNRS, Grenoble INP, IGE (Institute of Environmental Geosciences), 38000 Grenoble, France

Correspondence: Stuart K. Grange (stuart.grange@empa.ch); Christoph Hueglin (christoph.hueglin@empa.ch); Gaëlle Uzu (gaelle.uzu@ird.fr)

Abstract.

Particulate matter (PM) is the air pollutant that causes the greatest deleterious health effects across the world and PM is routinely monitored within air quality networks where PM mass according to its size, and sometimes number are reported. However, such measurements do not provide information on the biological toxicity of PM. Oxidative potential (OP) is a complementary metric

5 that aims to classify PM in respect to its oxidising ability in the lungs and is being increasingly reported due to its assumed relevance concerning human health. Between June 2018 and May 2019, an intensive filter-based PM sampling campaign was conducted across Switzerland in five locations which involved the quantification of a large number of PM constituents and OP for both PM_{10} and $PM_{2.5}$. OP was quantified by three assays: ascorbic acid (AA), dithiothreitol (DTT), and dichlorofluorescein (DCFH). OP_v (OP by air volume) was found to be variable in time and space with Bern-Bollwerk, an urban-traffic sampling site

10 having the greatest levels of OP_v among the Swiss sites (especially when considering OP_v^{AA}), with more rural locations such as Payerne experiencing lower OP_v. However, urban-background and suburban sites did experience significant OP_v enhancement, as did the rural Magadino-Cadenazzo site during wintertime because of high levels of wood smoke. The mean OP ranges for the sampling period were: 0.4–$4.1 \, \mathrm{nmol \, min^{-1} \, m^{-3}}$, 0.6–$3.0 \, \mathrm{nmol \, min^{-1} \, m^{-3}}$, and 0.3–$0.7 \, \mathrm{nmol \, H_2O_2 \, m^{-3}}$ for OP_v^{AA}, OP_v^{DTT}, and OP_v^{DCFH} respectively. A source allocation method using positive matrix factorisation (PMF) models indicated

15 that although all PM_{10} and $PM_{2.5}$ sources that were identified contributed to OP_v on average, the anthropogenic road traffic and wood combustion sources had the greatest OP_m potency (OP per PM mass). A dimensionality reduction procedure coupled to multiple linear regression modelling consistently identified a handful of metals usually associated with non-exhaust emissions, namely: copper, zinc, iron, tin, antimony and somewhat manganese and cadmium as well as three specific wood burning-sourced organic tracers – levoglucosan, mannosan, and galactosan (or their metal substitutes: rubidium and potassium) were

20 the most important PM components to explain and predict OP_v. The combination of a metal and a wood burning specific tracer led to the best performing linear models to explain OP_v. Interestingly, within the non-exhaust and wood combustion emission groups, the exact choice of component was not critical, the models simply required a variable to be present to represent the emission source or process. This analysis strongly suggests that the anthropogenic and locally emitted road traffic and wood

burning sources should be prioritised, targeted, and controlled to gain the most efficacious decrease in OP_v, and presumably biological harm reductions in Switzerland.

1 Introduction

1.1 Background

Particulate matter (PM) is a major atmospheric pollutant that is very diverse in terms of size, composition, solubility, and surface area. PM has deleterious effects on human health, reduces visibility, can negatively affect vegetation, and has significant climate effects (Harrison, 2020). With the resolution of the United Nations Human Rights Council stating that access to a clean, healthy, and sustainable environment is a human right (United Nations Human Rights Council, 2021), further understanding of PM and its negative health effects are required. These factors make PM a priority pollutant for management and control and thus, is widely monitored worldwide (World Health Organization, 2021). However, widespread routine PM monitoring is based primarily on mass within certain size fractions (and to a lesser extent, particle number) which contains no intrinsic information on sources or the potential for biological harm. There is evidence that carbonaceous species and transition metals are more toxic to biological systems than inorganic ions (Fang et al., 2017; Daellenbach et al., 2020; Leni et al., 2020). This gives rise to the motivation to define PM in terms of its biological reactivity and toxicity (Zhang et al., 2021).

The quantification of oxidative potential (OP) has the objective of being a "health-relevant" metric of ambient PM by conducting biological toxicological characterisation (Saffari et al., 2014; Borlaza et al., 2018; Bates et al., 2019). OP aims to complement PM mass and number monitoring data and is measured by quantifying the capacity of PM to drive oxidative stress after inhalation in target molecules, generally from the production of reactive oxygen species (ROS) (Delfino et al., 2013; Fang et al., 2016; Yadav and Phuleria, 2020). ROS are free radicals that are formed with molecular oxygen and such compounds can elicit inflammation responses and apoptosis (cell death), via complex triggers and cascades after inhalation, and therefore, presents a mechanism of biological toxicity caused by ambient PM (Bates et al., 2019). PM toxicity may result in inflammation, respiratory and cardiovascular diseases, cancer, and impediments to neural function (Raaschou-Nielsen et al., 2016; Liu et al., 2018a).

A number of toxicological assays have emerged that measure and quantify PM's OP, but to date, no standard definition has been decided on by consensus (Weber et al., 2018; Calas et al., 2019; Weber et al., 2021). However, the ascorbic acid (AA) and dithiothreitol (DTT) assays have emerged as potential standards to evaluate ROS and OP because of their relatively widespread use (Calas et al., 2017; Shirmohammadi et al., 2017; Yadav and Phuleria, 2020). However, due to the lack of standard operating procedures and calibrations, comparisons of OP measurements conducted by different laboratories is not advised, or at least should be done very cautiously (Janssen et al., 2014; Calas et al., 2018; Molina et al., 2020). OP is usually expressed in one of two ways: OP per volume of air (OP_v), or OP per PM mass (OP_m). OP_v is usually used for exposure studies because it is a metric that indicates the amount of OP a given population is exposed to. Contrasting this is OP_m which is a measure of PM's potency to cause OP per a given PM mass unit.

Previous research has indicated that the intrinsic OP_m of PM is highly variable and depends heavily on the constituents that make up the PM (Daellenbach et al., 2020). Such conclusions indicate that PM from some emission or generation sources have a greater capacity to drive OP_m (OP per µg). Transition metals (for example, iron, copper, and zinc) in particular have been repeatedly identified with correlation analyses as very potent OP_m drivers, which are generally sourced from road traffic, specifically non-exhaust emissions from tyre, brake, and road wear (Fang et al., 2016; Liu et al., 2018a; Bates et al., 2019; Taghvaee et al., 2019; Gao et al., 2020). Primary and secondary organic aerosol have also been identified as a potent driver of OP_m by some (Samake et al., 2017; Samaké et al., 2020), but because of the vast range of organics which can exist in the atmosphere, specific compounds have yet to be identified as the primary cause. Conversely, inorganic PM sources such as nitrate- and sulfate-rich sources as well as mineral dust have generally been found to have low OP_m (Daellenbach et al., 2020; Weber et al., 2021). This gives rise to a situation when investigating PM at a regional scale, the total mass distribution can be rather uniform, but OP is spatially highly heterogeneous (Yang et al., 2015; Liu et al., 2018b; Yu et al., 2021). This is because of the large contributions of inorganic compounds to mass, and the importance of very potent, but irregularly emitted constituents such as some metals near transport corridors and organics sourced from wood burning activities in specific communities, for example.

1.2 PM in Switzerland

Switzerland's ambient PM_{10} and $PM_{2.5}$ concentrations have progressively decreased since the mid-1990s after widespread monitoring began (Barmpadimos et al., 2011; Gianini et al., 2012; Grange et al., 2018; Hüglin and Grange, 2021). There is a strong site type gradient in Switzerland where rural locations are less polluted with PM when compared to roadside locations. However, woodburning remains popular in some locations, especially south of the Alps, and this can significantly elevate wintertime PM concentrations in these environments (Sandradewi et al., 2008; Grange et al., 2020). Based on recent intensive measurements, non-exhaust emissions from road vehicles is an emerging issue in Switzerland's urban areas. Brake wear, tyre wear, road wear, and resuspension of road dust have been shown to be important components of Switzerland's urban PM load (Hüglin and Grange, 2021; Grange et al., 2021; Rausch et al., 2022). Such emissions are generated by abrasive processes and although there is a tendency of such PM to be in the coarse-mode, these emissions can also significantly enhance fine PM concentrations. This is a result of the non-exhaust emission pathways generating PM with median diameters of approximately $3\,\mu m$ and thus, straddle the boundary between coarse and fine PM (Harrison et al., 2021). Non-exhaust PM is relevant in respect to OP because such particles are usually metal-rich and metals are thought to be very potent constituents for driving OP. Indeed, previous reports of OP in Switzerland demonstrated the importance of metals in the PM mix for enhanced OP (Yue et al., 2018; Daellenbach et al., 2020).

1.3 Objectives

The primary objective of this study is to describe Switzerland's ambient OP using observations from five sampling sites between 2018 and 2019. Additionally, two sub-objectives are identified: (*i*) to compare Switzerland's OP_v values with other locations where observations which can be robustly compared are available and, (*ii*) to use dimensionality reduction techniques,

explicitly, positive matrix factorisation (PMF) receptor models, random forest, and multiple linear regression models to identify what PM emission sources and components are most likely responsible for elevated OP (OP_v and OP_m). The implications of Switzerland's OP_v patterns and the identification of PM sources and constituents will be discussed with respect to PM and OP_v management.

2 Methods

2.1 Sampling sites

Daily PM filter samples were taken at five sampling sites across Switzerland (Table 1; Figure 1) between June 2018 and May 2019. The five monitoring sites used for the PM sampling are included in Switzerland's national air quality monitoring network; NABEL (Federal Office for the Environment, 2021). These established sites are used for compliance or regulatory monitoring and have long-term time series available for most common pollutants (Bundesamt für Umwelt, 2021). The sampling sites are located in different environments, ranging from rural to urban-traffic surrounds. One site, Magadino-Cadenazzo, is located south of the Alps while the other four are located on the Swiss Plateau.

Table 1. Basic information for the five monitoring sites in Switzerland which were used for oxidative potential PM measurements.

Site	Site name	Local ID	Canton	Lat.	Long.	Elev. (m)	Site type
ch0002r	Payerne	PAY	Vaud	46.8	6.9	489	Rural
ch0008a	Basel-Binningen	BAS	Basel-Landschaft	47.5	7.6	316	Suburban
ch0010a	Zürich-Kaserne	ZUE	Zürich	47.4	8.5	409	Urban
ch0031a	Bern-Bollwerk	BER	Bern/Berne	47.0	7.4	536	Urban-traffic
ch0033a	Magadino-Cadenazzo	MAG	Ticino	46.2	8.9	203	Rural

2.2 Data

High-volume PM_{10} and $PM_{2.5}$ quartz filter (Pallflex Tissuquartz 2500QAT-UP) samples were collected using Digitel DA-80H samplers with flow rates of $30\,m^3\,h^{-1}$. Daily sampling ran continuously from midnight and midnight for a 12-month period between June 1 2018 and May 31 2019. However, for the quantification of constituents beyond simple mass, punches from every fourth-days' filters were taken and analysed. Because the sites form part of the NABEL network, routine flow checks and various tests were regularly conducted in accordance to standard operating procedures.

In total, 908 filters were analysed with three OP assays. Eight-hundred and ninety-nine valid samples were reported, the missing samples were due to sampling or laboratory issues. Additional filter punches were used for a collection of other laboratory analyses to quantify other PM constituents such as elemental components (with inductively coupled plasma atomic emission spectrometry (ICP-AES) and inductively coupled plasma mass spectroscopy (ICP-MS)), ions (ion chromatography (IC)), elemental and organic carbon (thermal optical transmission (TOT) EN16909 method using the EUSAAR2 temperature protocol (European Committee for Standardization (CEN), 2017)), and a collection of additional organics (high-performance
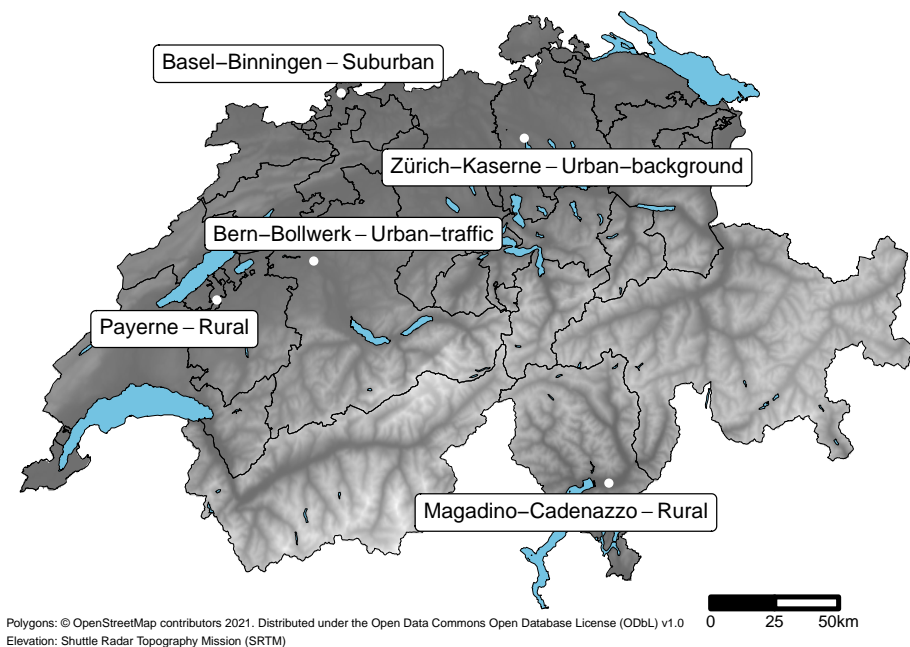
Figure 1. The five sampling sites in Switzerland that were used for oxidative potential PM measurements. The shading indicates the elevation of the terrain and filled blue areas show larger lakes and reservoirs. The cantonal boundaries are displayed as lines.

liquid chromatographic method followed by pulsed amperometric detection (HPLC-PAD)). The details of these additional methods have been reported previously by Hüglin and Grange (2021); Grange et al. (2021) and the latter publication can be

115 considered a companion to this paper. Grange et al. (2021) contains further descriptions of the five sampling sites and a more comprehensive overview of what chemical species were quantified.

2.3 Oxidative potential assays

OP was analysed with three different assays: ascorbic acid (AA), dithiothreitol (DTT), and dichlorofluorescein (DCFH). These analyses were conducted at the Institute of Environmental Geosciences, University of Grenoble Alpes, Grenoble, France. The

120 three different protocols are described in detail in Kelly and Mudway (2003); Cho et al. (2005); Calas et al. (2018, 2019).

PM samples were extracted using a simulated lung fluid (SLF) solution composed of a Gamble's and DPPC (dipalmitoylphosphatidylcholine) mixture. The Gamble's solution represents the interstitial fluid deep within lungs and is mixture of salts with a pH of 7.4. In order to maintain a constant amount of extracted PM, filter punches were adjusted by area to obtain an iso-mass of $25\,\mu g\,mL^{-1}$ to ensure intercomparison among the samples (Charrier and Anastasio, 2012; Calas et al., 2018).

125 Concentrations of $25\,\mu g\,mL^{-1}$ were used rather than $10\,\mu g\,mL^{-1}$ (as reported by Calas et al. (2018)) to enable the three assays to be conducted in parallel and to compensate for the DCFH assay's lower levels of sensitivity (Daellenbach et al., 2020). No

filtration was done in order to include both water-soluble and insoluble particles. Such an extraction method has been adopted to facilitate the extraction of PM in conditions closer to lung physiology (Calas et al., 2017).

The consumption of DTT in the assay was inferred as a measure of the ability of the PM to transfer electrons from DTT to oxygen, thereby producing reactive oxygen species (ROS). The PM extracts were reacted with DTT, resulting in the consumption of DTT in the solution. The remaining DTT was then titrated with 5,5-dithiobis-(2-nitrobenzoic acid) (DTNB) to produce a yellow chromophore (5-mercapto-2-nitrobenzoic acid or TNB), which was in direct proportion to the amount of reduced DTT remaining in solution after the reaction with the PM extract. The consumption of DTT ($\mathrm{nmol\,min^{-1}}$) was determined by following the TNB absorbance at 412 nm wavelength at 10 min intervals for a total of 30 min of analysis time.

The AA assay relies on one of the main lung antioxidants, ascorbic acid. The consumption of AA ($\mathrm{nmol\,min^{-1}}$) in the assay is inferred as the OP of PM quantified by the transfer of electrons from AA to oxygen, or the direct reaction between PM components and AA. Similar to the DTT assay, the PM extracts were reacted with AA into a UV-transparent well plate (CELLSTAR, Greiner-Bio). The absorbance was measured at 265 nm using a plate reader (TECAN spectrophotometer Infinite M200 Pro) at 4 min intervals for a total of 30 min of analysis time.

The 2,7-dichlorofluorescin (DCFH) assay is commonly used for detecting intracellular H_2O_2 and oxidative stress using a non-fluorescent probe through the formation of a fluorescent product (dichlorofluorescein or DCF) in the presence of ROS and horseradish peroxidase (HRP). DCF was measured by fluorescence at the excitation and emission wavelengths of 485 and 530 nm, respectively, every 2 min for a total of 30 min of analysis time. The ROS concentration in the sample is calculated in terms of H_2O_2 equivalent based on a H_2O_2 calibration (100, 200, 300, 400, 500, 1000, and 2000 nmol).

For all assays, the mixtures were injected into a 96-well plates and the absorbance was read from the microplate reader (TECAN spectrophotometer Infinite M200 pro). The well plates were shaken for 3 seconds before each measurement and kept at $37\,^{\circ}$C. Three laboratory blanks (in Gamble's + DPPC) and three positive controls (1,4-napthoquinone at $24.7\,\mathrm{\mu mol\,L^{-1}}$) were included in each plate. The average values of these blanks were subtracted from the sample measurements of the given plate. Detection limits (DL) were defined as three times the standard deviation of laboratory blank measurements. Uncertainties were estimated thanks to triplicate measurement of the same well.

The three assays have the same objective of determining the amount of oxidative stress an analyte can elicit, but the three assays have differing sensitivities to various components which form the PM mix and the specific antioxidants within the lung. The three assays have these general characteristics: AA is primarily sensitive to transition metals (Janssen et al., 2014), DTT is the most reported OP assay and is sensitive to organics and to a lesser extent, metals (Janssen et al., 2014; Calas et al., 2019), and DCFH shows a preferential sensitivity to a number of compounds that are often associated with secondary aerosol (Perrone et al., 2016; Pietrogrande et al., 2019). Therefore, the three assays give different perspectives on similar biological processes.

2.3.1 Units used

OP can be represented in two forms: OP per PM mass ($\mathrm{OP_m}$), or OP per volume of air ($\mathrm{OP_v}$). OP per volume of air is a superior unit when representing population exposure and therefore, this unit is mostly used in this analysis. There are three OP assays

reported and to differentiate these assays, a superscript notation is used, *i.e.*, OP_v^{AA}, OP_v^{DTT}, and OP_v^{DCFH}. For OP_v^{AA} and OP_v^{DTT}, the unit used is $\mathrm{nmol\,min^{-1}\,m^{-3}}$, while for OP_v^{DCFH}, the unit is $\mathrm{nmol\,H_2O_2\,m^{-3}}$.

2.4 Source apportionment

Source apportionment for PM_{10} and $PM_{2.5}$ for the five monitoring sites was conducted with the positive matrix factorisation (PMF) receptor model and the multilinear engine (ME-2) algorithm (Paatero and Tapper, 1994; Paatero, 1999). The PMF approach employed is informally known as "extended PMF" and was a result of the SOURCES research programme that involved the development of harmonised PMF methodology across several sites in France (Favez et al., 2017; Weber et al., 2019, 2021). The EPA PMF 5.0 software tool was used to apply PMF (Norris et al., 2014). Eight distinct factors/sources were identified for PM_{10}, while five sources were identified for $PM_{2.5}$. The PM_{10} sources were labelled as: sulfate-rich, nitrate-rich, road traffic, wood combustion, primary biogenic, secondary biogenic, mineral dust, and aged sea salt. For $PM_{2.5}$, the primary biogenic, mineral dust, and aged sea salt sources were not identified. Details on the specific settings, constraints, and process of the extended PMF modelling can be found in the accompanying Grange et al. (2021) publication. The PMF input and output data are also available in a persistent data repository for others' convenience (Grange, 2021a).

The PMF analysis for the particular dataset was challenging because of the existence of fewer than the recommended samples available (91 compared to the recommended at least 100 ht(Norris et al., 2014)), low signal to noise ratios for many variables because of low ambient concentrations, and the inclusion of extra organic species into the PMF models. Despite the many validation steps conducted, the models had a number of limitations which are discussed fully in the companion paper Grange et al. (2021) and were considered in the current work.

2.5 Linking PM sources to OP

The OP measurements were not included in the PMF modelling process, but these observations required linking to the PMF-identified sources. To estimate the source contributions to the three OP assays, weighted robust multiple linear regression (MLR) with an iterative M-estimator was used. Conceptually, the OP observations were explained by the PMF-identified sources, and because linear regression models return coefficients in the dependent variable's response scale, the estimates of the PMF-identified sources for OP are readily interpreted by investigating the models' slope coefficients (β). The equation expressing this process can be found elsewhere (Weber et al., 2021, Equation 4). To allow for evaluation of the models' coefficients' uncertainty, the data were bootstrapped 500 times and modelled. Additionally, the OP's analytical uncertainties were included in the models as weights. The **MASS** R package was used as the interface to the robust linear regression function (Venables and Ripley, 2002). An example of how this process was conducted can be found in a public repository (Grange, 2021c).

2.6 OP modelling

The filter-based measurement campaign resulted in a large number of elements, ions, and organics to be quantified which compose Switzerland's PM. To extract the constituents which were the most important for OP, a multiple-step process was conducted to firstly identify the most important constituents which explain OP and secondly, what combination of these constituents resulted in the best statistical models which explained OP values in Switzerland.

The identification of the most important PM constituents to explain OP was conducted with random forest, an ensemble decision tree machine learning algorithm (Breiman, 2001; Wright and Ziegler, 2017). The entire set of variables available was used to model OP. The random forests' importances for the included variables were extracted and analysed to reduce the feature space (Abdulhammed et al., 2019; Reddy et al., 2020). Variable importance is a metric that represents the improvement of information gain at each split in the decision tree for a particular independent variable. Therefore, variable importance aids the determination of a subset of useful variables. Permutation variable importance approach was the specific algorithm used and this approach evaluates prediction accuracy with the sampled (out-of-bag; OOB) observations and permuting each variables' values to determine the effect on prediction performance (Wright et al., 2016).

The variables that were consistently identified as the top 12 most important for the explanation of OP_v^{AA} and OP_v^{DTT} by random forest were used in further linear modelling work. This dimensionality reduction pre-processing step allowed the dataset to be reduced from over 50 variables to the most important ≈ 15 for two OP assays. The sets of the top 12 variables differed slightly among the different sites, PM size fractions, and OP assays, hence the identified variables were not identical across all groups.

The most important variables identified by random forest were used to model OP with robust multiple linear regression (Venables and Ripley, 2002). Individual models using all combinations of the ≈ 15 variables with a maximum of five predictors were created to explain OP_v. The intercept term was excluded from the model formulation and over $100\,000$ models were calculated. An example of how this was achieved is accessible via a public repository (Grange, 2021b). To identify models which were suitable for further use, three filters were applied to the models. Models with a maximum pairwise variance inflation factor (VIF) for independent variables greater than 2.5 were removed because this suggests multicollinearity among the independent variables (Jackson et al., 2009). Models which contained negative term estimates were also dropped, as were models with R^2 values less than 75 %. These filters resulted in 371 models to be kept for further analysis and the majority (77 %) of these models had two independent variables.

3 Results and discussion

3.1 Spatial-temporal variation of OP

OP measurements between June, 2018 and May, 2019 at five sampling locations throughout Switzerland demonstrated that OP_v was variable in both time and space. Mean OP_v almost always increased as the sampling location became increasingly urban and Bern-Bollwerk, an urban-traffic site, had the highest levels of OP_v during the sampling period while Payerne, a rural

location had the lowest mean OP_v (Figure 2; Table 2). For OP_v^{AA}, the PM_{10} means ranged from 0.7 and 4.1 $\mathrm{nmol\,min^{-1}\,m^{-3}}$ and for $PM_{2.5}$, the corresponding range was 0.4 and 1.6 $\mathrm{nmol\,min^{-1}\,m^{-3}}$. OP_v^{DTT} means ranged from 0.8–3.0 and 0.6–1.1 $\mathrm{nmol\,min^{-1}\,m^{-3}}$ for PM_{10} and $PM_{2.5}$ respectively. OP_v^{DCFH} did not show the same progressive increase across the rural to urban roadside gradient with another rural site, Magadino-Cadenazzo having the highest means (0.7 $\mathrm{nmol\,H_2O_2\,m^{-3}}$ for both PM_{10} and $PM_{2.5}$) while the other four sites were inconsistently ranked for the different PM size fractions and considering the different types of averages (Table 2). The rural-urban-roadside gradient observed for OP_v^{AA} and OP_v^{DTT} was also demonstrated by PM mass and most other individual constituents (the exception was secondary components such as nitrate, sulfate, and ammonium) which form the Swiss PM mix, and this has been reported previously in a companion paper (Grange et al., 2021).
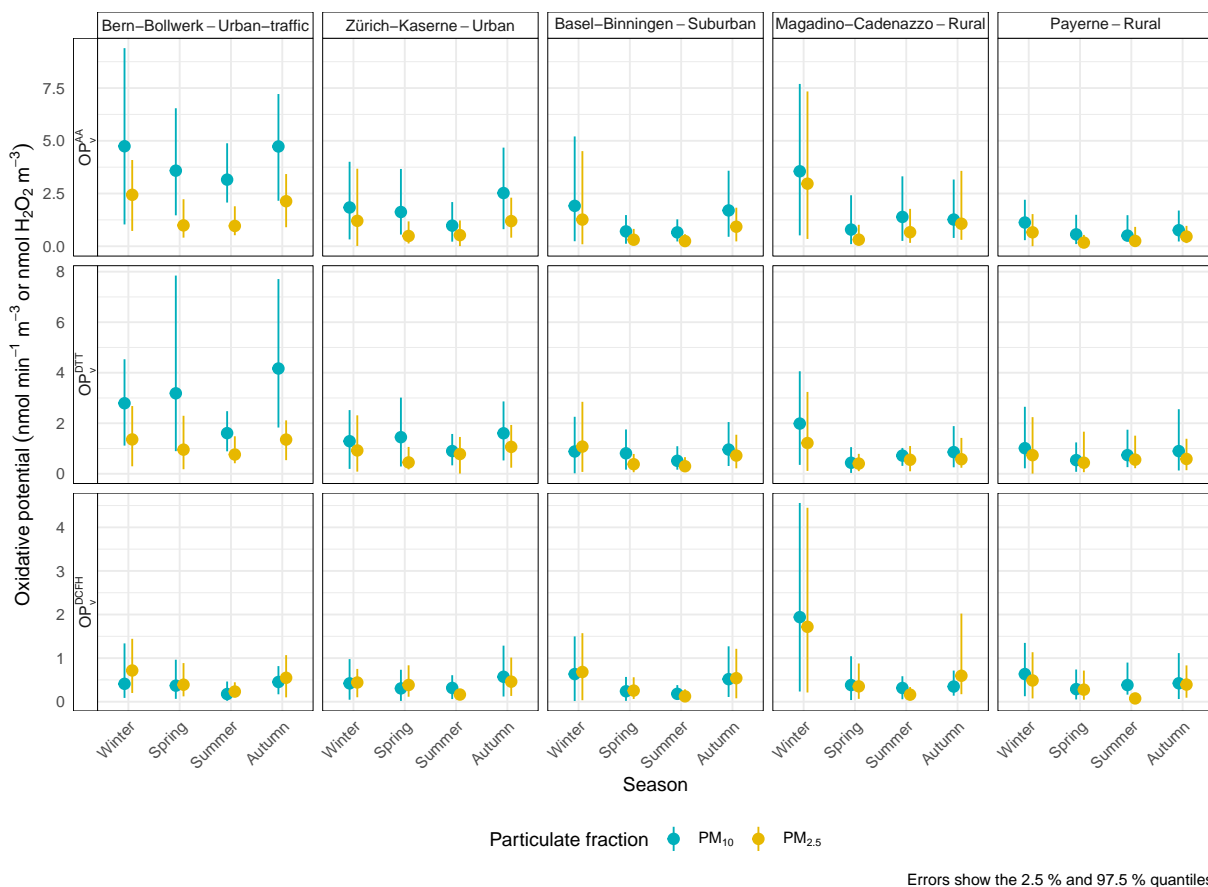
Figure 2. Seasonal means of three OP_v assays, two PM size fractions, and five sampling sites in Switzerland between June, 2018 and May, 2019.

Winter and autumn had the highest average OP which is consistent with the common winter situation where primary atmospheric pollutants emissions are higher, and the atmospheric state is less conducive to pollutant transportation and dispersion (Beyrich, 1997; Emeis and Schäfer, 2006). The wintertime OP enhancement was especially clear at Magadino-Cadenazzo, a

Table 2. Simple summary statistics for three OP_v assays, two PM size fractions, and five sampling sites in Switzerland between June, 2018 and May, 2019. $\bar{x}$ and M represent the mean and median respectively while lower and upper refer to the 2.5 % and 97.5 % quantiles (which contain 95 % of the observations). The summaries have been rounded to one decimal point and the units are $\mathrm{nmol\,min^{-1}\,m^{-3}}$ for OP_v^{AA} and OP_v^{DTT} and $\mathrm{nmol\,H_2O_2\,m^{-3}}$ for OP_v^{DCFH}.

PM	Site	OP_v^{AA}				OP_v^{DTT}				OP_v^{DCFH}			
		$\bar{x}$	M	Lower	Upper	$\bar{x}$	M	Lower	Upper	$\bar{x}$	M	Lower	Upper
PM_{10}	Bern-Bollwerk	4.1	3.8	1.3	8.4	3.0	2.6	0.9	7.6	0.4	0.3	0.0	0.9
PM_{10}	Zürich-Kaserne	1.7	1.4	0.4	4.5	1.3	1.1	0.3	2.9	0.4	0.3	0.0	1.1
PM_{10}	Basel-Binningen	1.2	0.9	0.2	3.3	0.8	0.7	0.1	1.9	0.4	0.3	0.0	1.3
PM_{10}	Magadino-Cadenazzo	1.7	1.2	0.2	5.5	1.0	0.8	0.1	3.3	0.7	0.4	0.1	3.2
PM_{10}	Payerne	0.7	0.6	0.1	2.2	0.8	0.7	0.1	2.4	0.4	0.3	0.1	1.1
$PM_{2.5}$	Bern-Bollwerk	1.6	1.4	0.5	3.8	1.1	0.9	0.2	2.2	0.5	0.3	0.1	1.1
$PM_{2.5}$	Zürich-Kaserne	0.8	0.6	0.0	2.5	0.8	0.8	0.0	2.1	0.4	0.3	0.1	0.8
$PM_{2.5}$	Basel-Binningen	0.7	0.4	0.1	1.9	0.6	0.4	0.1	2.0	0.4	0.2	0.0	1.3
$PM_{2.5}$	Magadino-Cadenazzo	1.2	0.6	0.0	5.0	0.7	0.5	0.1	2.0	0.7	0.3	0.1	2.7
$PM_{2.5}$	Payerne	0.4	0.3	0.0	1.2	0.6	0.5	0.0	1.7	0.3	0.2	0.0	0.9

site known to be heavily burdened by wood smoke during the winter months (Grange et al., 2020). Notably, at Magadino-Cadenazzo, wintertime $PM_{2.5}$ OP_v was enhanced to nearly the same extent as PM_{10} because of wood burning sourced PM being almost all contained in the fine-mode (Kleeman et al., 1999). Bern-Bollwerk was clearly the most polluted site with respect to OP_v where the two AA and DTT assays remained elevated for all seasons, but mean OP_v^{DTT} was significantly lower during the summer than in the other seasons. Another key observation from these aggregations was that PM_{coarse}, defined as the mass concentration of PM with a size between 2.5 and 10 μm, contained 50 and 45 % of the OP_v^{AA} and OP_v^{DTT} signal respectively. This was only able to be highlighted because the sampling design included both PM_{10} and $PM_{2.5}$. This point implies that PM_{coarse} is potentially relevant for human health and for regulatory purposes. Therefore, it is important to continue PM_{10} monitoring in addition to the measurement of $PM_{2.5}$.

Figure 2 and Table 2 shows large differences among the three assays used to quantify OP_v in this work. The DCFH assay based on a fluorescence method showed much lower levels of spatial and seasonal variation when compared to the other two, more established AA and DTT assays where the means ranged between 0.3 and 0.7 $\mathrm{nmol\,min^{-1}\,m^{-3}}$ (Figure A1). The DCFH assay has a lower level of sensitivity when compared to the AA and DTT assays, nevertheless, the sensitivity of DCFH to organic-rich PM was observed at the southern Magadino-Cadenazzo sampling location where OP_v enhancement was clear during the winter because of high concentrations of wood burning emissions. The AA assay is primarily sensitive to metals (Janssen et al., 2014), and the Bern-Bollwerk site which is known to experience significant non-exhaust emissions from road traffic, observed high levels of OP_v^{AA} during the sampling period and the mean was 4.1 $\mathrm{nmol\,min^{-1}\,m^{-3}}$. Less severe enhancements were also observed for the urban and suburban Zürich-Kaserne and Basel-Binningen sites with the AA assay suggesting some metal contamination of these atmospheres too. These observations are consistent with work exploring the

urban and roadside increments in Switzerland, and the importance of non-exhaust emissions to these increments (Grange et al., 2021).

3.1.1 OP comparison with other locations

The comparison of OP metrics among different locations and sampling durations is problematic due to the lack of standardised OP laboratory procedures (Calas et al., 2019). Here, however, comparisons can be made with many French sites where OP_v has been quantified by the same laboratory with identical analytical approaches. The OP_v of $PM_{2.5}$ has been rarely reported in Europe, and therefore, only PM_{10}'s OP_v will be discussed here. Additionally, comparisons of the DCFH assay were unable to be conducted due to a lack of available data for the French sites.

Based on Weber et al. (2021) which consolidated annual OP_v data for 14 sampling sites across France between 2013 and 2018, Bern-Bollwerk's atmosphere had high levels of OP_v – especially when considering OP_v^{AA} (Table A1). Bern-Bollwerk's PM_{10} OP_v^{AA} mean of $4.1\,\mathrm{nmol\,min^{-1}\,m^{-3}}$ was substantially higher than all other French sampling locations with the second most polluted location being in Chamonix (site code CHAM), a town in an alpine valley which is topographically confined and where the annual mean OP_v^{AA} was reported as $2.6\,\mathrm{nmol\,min^{-1}\,m^{-3}}$ (between November 2013 and October 2014). The four other Swiss sites were within the same range of the reported values for the French locations, however, both Zürich-Kaserne and Magadino-Cadenazzo were ranked in the upper half of mean OP_v^{AA} when comparing the 19 sites (14 in France and five in Switzerland). A map of seasonal and annual OP_v^{AA} and OP^{DTT} means for the closest French sites surrounding Switzerland and the five Swiss sites included in this analysis are shown in Figure 3.

Bern-Bollwerk also demonstrated high levels of OP_v^{DTT} when compared to the other sampling locations, but for this metric, Chamonix was more polluted than Bern-Bollwerk with means of 4.4 and $2.9\,\mathrm{nmol\,min^{-1}\,m^{-3}}$ respectively (Table A1; Figure 3). The Basel-Binningen, Payerne, and Magadino-Cadenazzo Swiss sites had the lowest OP_v^{DTT} means when considering the 19 sites that suggests that Switzerland has generally lower levels of OP_v^{DTT} than France, which can be contrasted with OP_v^{AA}, where concentrations experienced in Switzerland were similar to those reported across France.
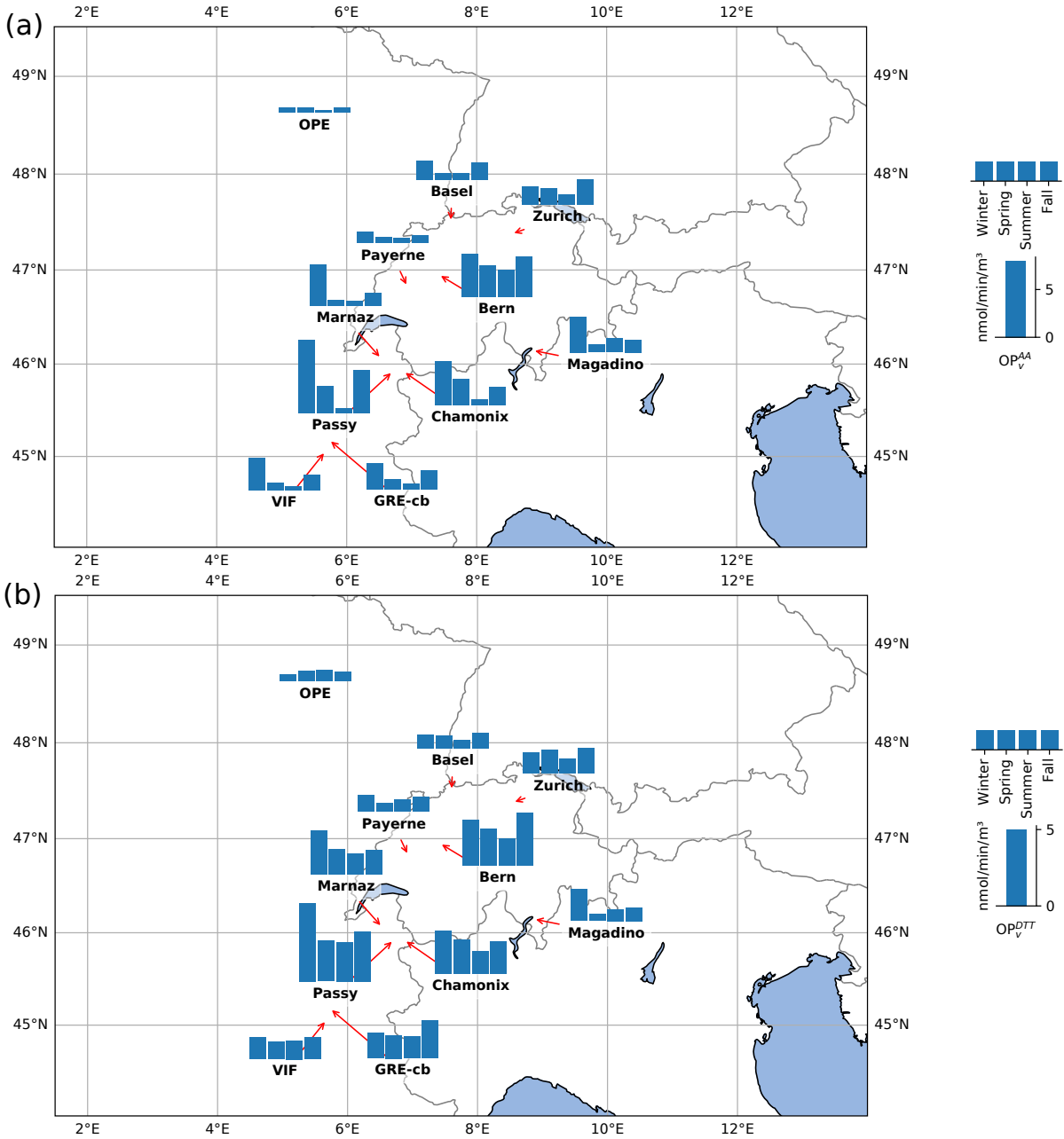
Figure 3. Seasonal OP_v^{AA} (a) and OP_v^{DTT} (b) PM_{10} means for five Swiss sites included in this analysis and the closest six French sites surrounding Switzerland. Data from the French sampling sites are from Weber et al. (2021).

3.2 Linking OP to PM sources

The PMF source apportionment analysis identified eight PM sources in Switzerland: sulfate-rich, nitrate-rich, road traffic, wood combustion, primary biogenic, secondary biogenic, mineral dust, and aged sea salt. All the eight sources were detected for PM_{10} while the primary biogenic, mineral dust, and aged sea salt sources were not identified in the $PM_{2.5}$ fraction indicating that these sources were mostly in the coarse-mode. A full discussion of the PMF results, the limitations, and the sources' characteristics can be found in the companion paper, Grange et al. (2021), however, an outline of the PMF results is briefly given below.

The PMF results indicated that about 50 % of the PM_{10} and $PM_{2.5}$ load in Switzerland was from the three predominantly secondary nitrate-rich, sulfate-rich, and aged sea salt sources. Based on the models' factor/source profiles, the former two sources contained a significant amount of organic mass. Generally, the primary and secondary biogenic sources were rather low contributors to average PM_{10} mass concentrations (8.9 % to 15.8 %), but they were highly seasonal sources and the secondary biogenic source was more important for $PM_{2.5}$ (13.8 % to 23.0 %) than PM_{10}. The wood burning, mineral dust, and road traffic sources were more enhanced in urban areas, but their enhancement was highly dependent on the sites' immediate environmental surrounds. Bern-Bollwerk's road traffic source contributed more than a third to both PM_{10} and $PM_{2.5}$, while the wood burning source contributed over 20 % to both PM fractions at Magadino-Cadenazzo, despite being a source which was inactive for about half of the sampling period.

To investigate the relationship between the activities of the identified main PM sources in Switzerland on its OP, the PMF sources were used in conjunction with OP_v observations. OP_v was explained using MLR models for each of the five sites with the identified PMF source contributions as independent variables (in $\mu g \, m^{-3}$). The units of the estimated model coefficients for the PM sources were then in $nmol \, min^{-1} \, \mu g^{-1}$ and interpreted as the intrinsic OP_m. This process has been called an 'inversion' by others (Weber et al., 2021; Borlaza et al., 2021) and was conducted 500 times with bootstrapped inputs for each site, assay, and PM size fraction to allow for robust estimates of the models' terms. When considering the sets' model residuals, they were normality distributed and the mean R^2 for OP_{AA} and OP_{DTT} models were 87 and 80 % respectively. The lack of structure in the DCFH observations (Figure A1) resulted in poorly performing models and therefore, this assay was not included in further analyses.

When the explanatory multiple linear regression models were exposed to the PMF-identified sources it was clear that the anthropogenic road traffic and wood combustion sources had the greatest intrinsic OP_m (Figure 4). When combining the five sites' results together, the road traffic and wood combustion sources were always the highest ranked OP_m sources, with the exception of DTT for $PM_{2.5}$ where wood combustion was ranked first, but road traffic fell to fourth place and the nitrate-rich source was placed second. The metal-sensitive AA assay showed that the coarse-mode road traffic source was the most potent PM source in Switzerland giving additional evidence that coarse, non-exhaust emissions drove this assay's OP_m results. The mostly fine and carbonaceous wood combustion source was always important for the two OP_m assays and was clearly the most potent source for $PM_{2.5}$. The other remaining six sources had, on average, positive contributions to OP_m, but were far less important for OP_m when compared to the road traffic and wood combustion sources based on this analysis. Notably, the nitrate- and sulfate-rich sources generally showed low levels of OP_m which outlines a disconnect between average PM

mass concentrations and OP_m potency. This suggests that all PM has the ability to contribute to OP, but road traffic and wood combustion source are the two sources that should be prioritised for control and management to efficiently reduce OP_v in Switzerland. Unlike Samake et al. (2017); Weber et al. (2021), these results do not suggest that biogenic-sourced PM is particularly important for OP_m in Switzerland, perhaps due to different fungal and plant species found in different environments or the differing intensities of agriculture and cultivation between the two countries (Samaké et al., 2019; Samake et al., 2017).

310
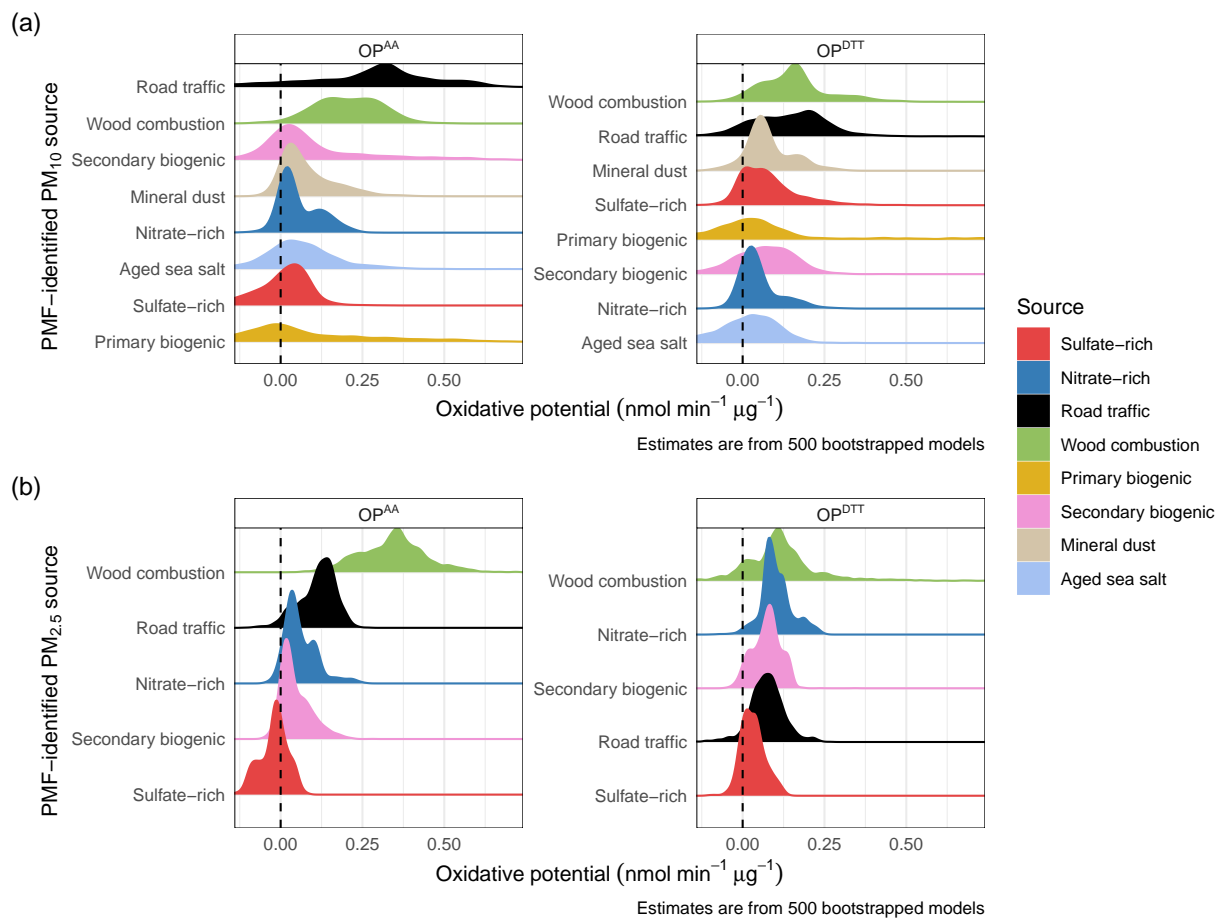
Figure 4. Densities of the intrinsic OP_m^{AA} (a) and OP_m^{DTT} (b) estimates for the eight PM_{10} and five $PM_{2.5}$ PMF-identified sources. The estimates for all five sites included in the analysis have been aggregated.

3.3 Identifying important PM constituents with random forest

Within the PMF-identified sources shown in Figure 4, there are a large number of constituents that give the sources their characteristics. To better identify the specific components which compose the PM sources identified in Switzerland that were important and potent drivers of OP_v, presumably, mostly contained within the road traffic and wood combustion sources, a

315

multi-step modelling process was conducted. The random forest algorithm was used to calculate variable importance and all variables included in the data set were ranked (Breiman, 2001). A high importance ranking indicates that the variable is more important for the dependent variable's explanation and the utilisation of the random forest algorithm for this sort of application has gained traction in many fields (Behnamian et al., 2019). The motivation for this process was to simplify and resolve the lower-level linkages between PM components and OP_v when the PMF sources were potentially heterogeneous among the sampling sites and PM size fractions.

When the random forest importances were calculated for each site, PM fraction, and OP_v assay, it was clear that a collection of organics and metals were commonly identified as being the most important variables for the explanation of OP_v. Elements and organic compounds associated with wood combustion: rubidium (Kleeman et al., 1999; Reid et al., 2005; Svane et al., 2005), potassium, levoglucosan, mannosan and galactosan (Urban et al., 2012) were constantly ranked highly in terms of importance (Figure 5). The other group of components which were identified were metals such as copper, zinc, iron, tin, antimony, and to some extent manganese and cadmium. This collection of metals is usually associated with vehicular non-exhaust emissions and is generated by abrasive or wear processes (Charron et al., 2019; Harrison et al., 2021). EC and OC were also commonly identified and these variables are associated with both wood burning and vehicle exhaust emissions. Despite these two groups of PM constituents being identified, both mass and ions (especially nitrate) were also present in the most important variables identified by random forest. We interpret the presence of these variables as proxies of total PM mass indicating that although for a given PM mass, OP_v may vary depending on its make-up, total PM mass is still an important, and related metric. Therefore, the importance analysis was consistent with the PMF inversion process discussed in Section 3.2.

Figure 5 also shows some site-specific variation due to the sites' different local emissions. For example, in Bern-Bollwerk, the non-exhaust sourced metals such as copper, iron, and zinc were ranked higher than the mean importance rank across the five sites. This feature was present in both assays and was somewhat clearer in PM_{10} due to the tendency of abrasive processes to emit PM larger than $2.5\,\mu m$ (Harrison et al., 2021). Magadino-Cadenazzo on the other hand demonstrated a tendency of rubidium, potassium, mannosan, and levoglucosan to be more important than the sites' mean ranking which was consistent with what is known about this site's exposure to local emissions because it experiences a heavy wood smoke load (Sandradewi et al., 2008; Chen et al., 2021). When comparing the two PM size fractions, there was no clear dominating source and the differences between PM_{10} and $PM_{2.5}$ were overshadowed by site-specific differences. This supports the conclusions made in a companion paper (Grange et al., 2021) where non-exhaust $PM_{2.5}$ emissions were found to be considerable and are important to consider across the Swiss sampling sites. When exposing the PMF sources (eight for PM_{10} and five for $PM_{2.5}$) to the same random forest importance analysis, the road traffic and wood combustion sources were clearly the most important sources for OP explanation, as shown in Figure 4.

A slightly different representation of the random forest importance rankings is provided in Figure 6, where the presence of variables in the group was considered highly important were counted for the five sites, two OP_v assays, and two PM fractions. In this case, highly important variables were defined as the top 12 variables. It is noticeable that rubidium and copper, two tracers for wood burning and non-exhaust emissions, were ranked as the most important variables for PM_{10} at all five sites and for both OP_v assays. For $PM_{2.5}$, where concentrations of many metals were lower than in PM_{10}, only a wood burning tracer
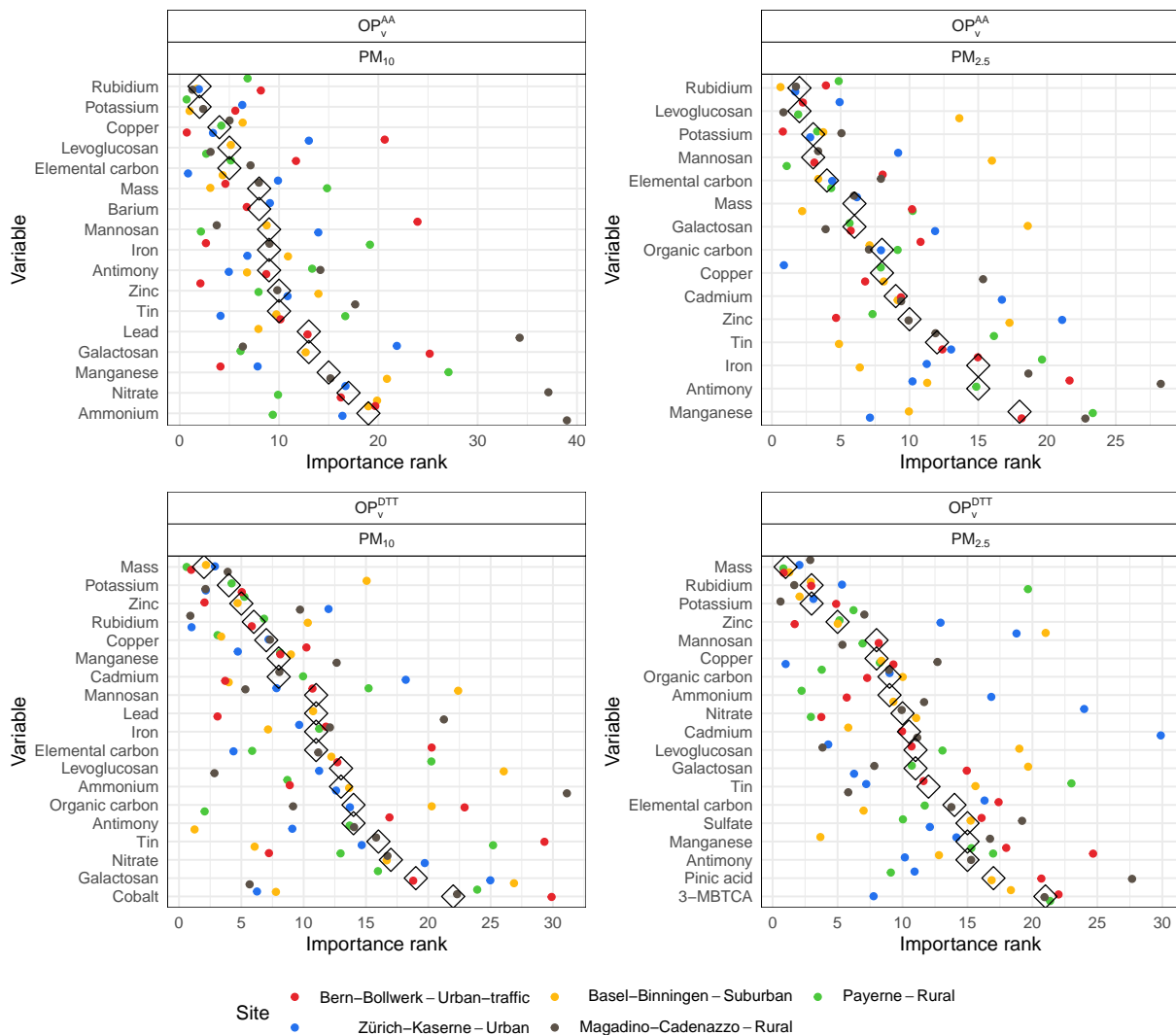
Figure 5. Random forest importance plot of the top independent variables for two OP$_v$ assays, two particulate size fractions, and five sampling sites. The large open diamonds represent the variables' medians and the variables are ordered by their median ranking.

(either potassium or rubidium) together with PM mass were identified across all five sites and both OP$_v$ assays. All variables which were identified more than once for each OP$_v$ assay and PM size fraction (the variables shown in the y-axes of Figure 6) were used in the next step of linear modelling to identify what variables are best to be used when forming predictive models to explain OP$_v$.
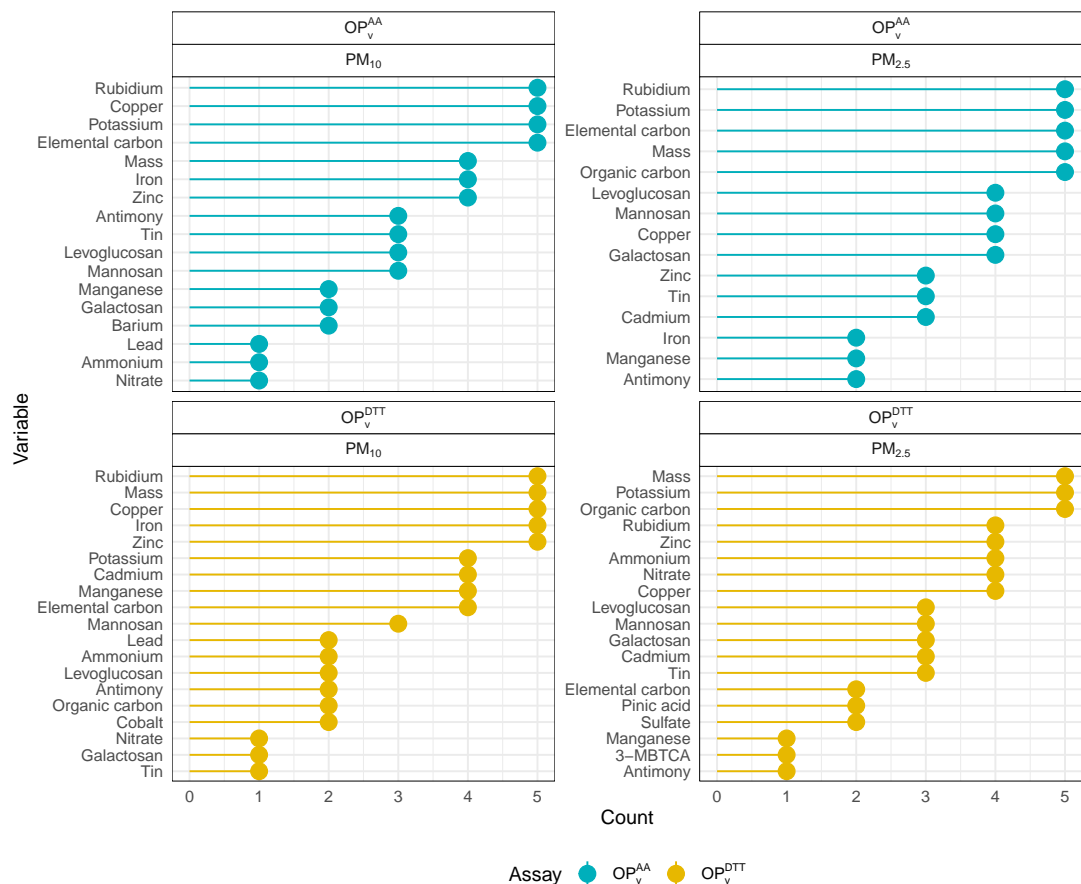
Figure 6. Counts of how many times an independent variable was ranked highly (within the top 12) in terms of random forest importance for two OP$_v$ assays, two particulate size fractions, and five sampling sites. Variables with counts of five shows that for every site included in the analysis, this variable was identified as important for the explanation of OP$_v$.

3.4 Modelling OP

The most important variables at each site, identified by the rank of the random forest importance (Figure 6), were used to build multiple linear regression models to explain OP_v. Every combination of the variables were used to calculate linear regression models (with a maximum of five independent variables and the intercept terms omitted) and after training, only the models with positive slope estimates, those which had a maximum pairwise variance inflation factor (VIF) of less-than 2.5, and had an R^2 greater-than 75 % were kept. These three filters ensured the models selected did not suffer from undesirable levels of multicollinearity among their independent variables (Jackson et al., 2009; Barmpadimos et al., 2011) and performed adequately on their training set. The VIF filter removed all models with more than four independent variables due to the increased probability of multicollinearity when including additional independent variables in the same model. A total of 100 342 models were trained and 371 models passed the filters. The number of models trained for each site, PM fraction, and OP assay is shown in Table A2.

When analysing the models with the best performance based on their R^2 values, 77 % had two independent variables while models with one or three independent variables only composed 13 % and 10 % of the total set. Almost without exception, the best models' independent variables included a metal and an organic compound. The metals contained in the models were the same as those identified and discussed previously (Figure 5; Figure 6) and are generally emitted from abrasive processes related to road vehicles (iron, zinc, copper, antimony, but also cadmium), while the organics were the specific biomass burning markers of levoglucosan, mannosan, and galactosan. Table 3 shows equations of the best performing models based on their R^2 values for each sampling site, the two PM size fractions and the two OP_v. However, all models fulfilling the applied filter criteria can be considered appropriate and considered as suitable models for explaining the observed OP_v. The full list of these suitable models is provided in the Supplementary Information (Table S1), the counts of all pairwise combinations of variables in the suitable models with two or more independent variables are shown in Figure 7.

The best performing models demonstrated that the *combination* of vehicular non-exhaust emission and wood burning tracers were required to generate the best models to explain OP_v. Interestingly, the exact tracers or markers used for the modelling were not critical. For example, using antimony, copper, or iron as the representative non-exhaust emission species resulted in models which performed very similarly and showed that these three metals were effectively interchangeable with one another. Cadmium, manganese, and zinc could also be added to this group, but the use of these metals resulted in models which performed slightly worse on average and such patterns may be related to the different elements' analytical detection limits or the multiple emission sources these metals have. The same phenomenon was present for the wood burning tracers of levoglucosan, mannosan, and galactosan where the selection of one of these organics over the other was not critical for the explanation of OP_v.

Figure 7 shows, that the combinations of independent variables in the suitable models for explaining OP_v^{AA} are different from those for explaining OP_v^{DTT}. There is clearly a larger number of combinations of independent variables in the models for OP_v^{AA} compared to OP_v^{DTT}. The combinations of selected variables in models for OP_v^{AA} are for both PM size fractions predominantly the above-mentioned pairs of tracers for vehicular non-exhaust and wood burning emissions. It is interesting

Table 3. The best performing robust multiple linear regression model equations for each site, two PM fractions, and two OP_v assays. The units used for the independent variables are $\mu g\,m^{-3}$.

PM	Site	OP assay	R^2 (%)	Equation
PM_{10}	Payerne	OP_v^{AA}	87	$OP_v = 106.52(\text{galactosan}) + 2.78(\text{iron})$
PM_{10}	Magadino-Cadenazzo	OP_v^{AA}	95	$OP_v = 1.93(\text{levoglucosan}) + 2.6(\text{iron})$
PM_{10}	Basel-Binningen	OP_v^{AA}	96	$OP_v = 95.89(\text{galactosan}) + 130.38(\text{copper})$
PM_{10}	Zürich-Kaserne	OP_v^{AA}	91	$OP_v = 41.72(\text{mannosan}) + 750.09(\text{antimony})$
PM_{10}	Bern-Bollwerk	OP_v^{AA}	89	$OP_v = 109.01(\text{galactosan}) + 318.68(\text{manganese})$
PM_{10}	Payerne	OP_v^{DTT}	86	$OP_v = 151.44(\text{manganese}) + 0.32(\text{ammonium})$
PM_{10}	Magadino-Cadenazzo	OP_v^{DTT}	87	$OP_v = 11.81(\text{mannosan}) + 134.34(\text{manganese})$
PM_{10}	Basel-Binningen	OP_v^{DTT}	90	$OP_v = 1.53(\text{iron}) + 0.44(\text{ammonium})$
PM_{10}	Zürich-Kaserne	OP_v^{DTT}	79	$OP_v = 3.12(\text{potassium}) + 0.24(\text{OC})$
PM_{10}	Bern-Bollwerk	OP_v^{DTT}	80	$OP_v = 2(\text{EC}) + 0.85(\text{ammonium})$
$PM_{2.5}$	Payerne	OP_v^{AA}	90	$OP_v = 2.51(\text{levoglucosan}) + 88.29(\text{copper})$
$PM_{2.5}$	Magadino-Cadenazzo	OP_v^{AA}	97	$OP_v = 23.04(\text{mannosan}) + 3.98(\text{iron})$
$PM_{2.5}$	Basel-Binningen	OP_v^{AA}	88	$OP_v = 2.53(\text{levoglucosan}) + 613.81(\text{antimony})$
$PM_{2.5}$	Zürich-Kaserne	OP_v^{AA}	91	$OP_v = 2.91(\text{levoglucosan}) + 107.98(\text{copper})$
$PM_{2.5}$	Bern-Bollwerk	OP_v^{AA}	90	$OP_v = 17.73(\text{mannosan}) + 107.21(\text{copper})$
$PM_{2.5}$	Payerne	OP_v^{DTT}	93	$OP_v = 0.19(\text{organic\_carbon}) + 0.1(\text{nitrate})$
$PM_{2.5}$	Magadino-Cadenazzo	OP_v^{DTT}	85	$OP_v = 8.25(\text{galactosan}) + 0.06(\text{mass})$
$PM_{2.5}$	Basel-Binningen	OP_v^{DTT}	89	$OP_v = 17.9(\text{galactosan}) + 129.44(\text{copper}) + 0.08(\text{nitrate})$
$PM_{2.5}$	Zürich-Kaserne	OP_v^{DTT}	84	$OP_v = 2.45(\text{potassium}) + 0.19(\text{ammonium}) + 70.49(\text{pinic acid})$
$PM_{2.5}$	Bern-Bollwerk	OP_v^{DTT}	88	$OP_v = 30.91(\text{galactosan}) + 474.89(\text{tin}) + 0.34(\text{ammonium})$

to note that although rubidium and potassium had higher ranks in the random forest importance, the suitable models for explaining mostly included an organic tracer for wood burning emissions (levoglucosan, mannosan, or galactosan). This could be explained by rubidium and potassium having multiple emission sources and therefore were removed by the multicollinearity filter used for the model selection.

We interpret the presence of levoglucosan, mannosan, and galactosan in this analysis as simply indicators of biomass burning emission sources. This is because these particular organic compounds are not redox-active and therefore, they cannot be the components of PM that drove OP. Quinones, rubidium, and/or other co-emitted products from biomass burning are most likely the responsible components, and this is a clear example of how an observational study can suggest and highlight associations or correlations, but not necessarily causality.

In contrast to OP_v^{AA}, PM mass or ammonium and nitrate were present in the better performing models for OP_v^{DTT} at times. It is unlikely that ammonium and nitrate are indeed strong drivers of OP_v since ammonium sulfate and nitrate (($NH_4)_2SO_4$ and NH_4NO_3) have been shown to have negligible OP (Daellenbach et al., 2020), the presence of these inorganic ions might
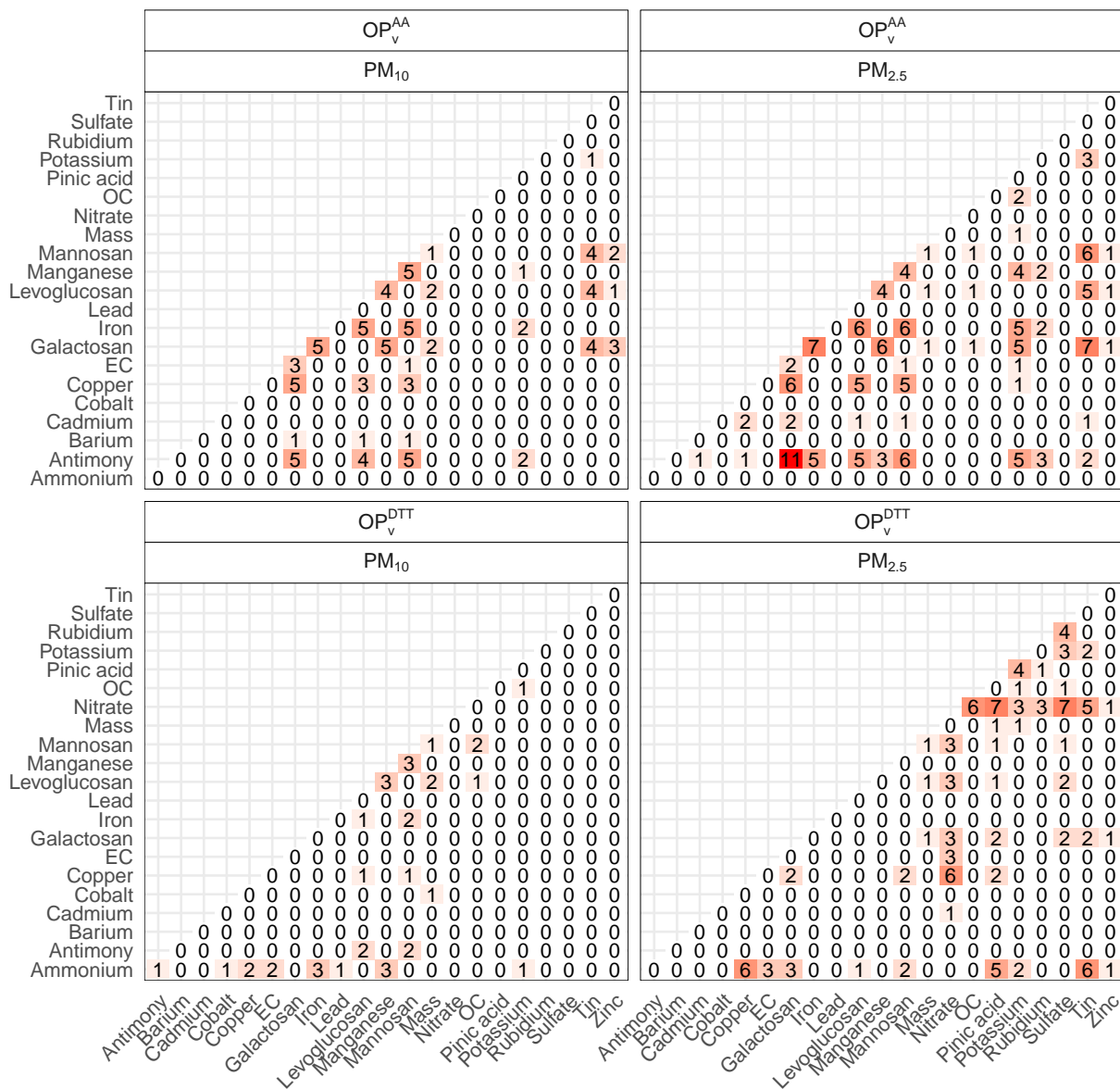
Figure 7. Number of times when a combination of two independent variables for the filtered models were present for PM$_{10}$ and PM$_{2.5}$ and two OP$_v$ assays for five sampling sites.

be acting as a proxy for total ambient PM concentrations or perhaps seasonal emission cycles due to its shift between gas and aerosol phases in the different seasons because of changes in ambient air temperature. For PM$_{2.5}$'s OP$_v^{\text{DTT}}$, OC as well as pinic acid (a tracer for biogenic secondary organic aerosol) were frequently found in the 371 models which passed the model selection criteria. OC and pinic acid might also be understood as proxies for total PM concentrations or specific conditions

405 leading to elevated PM levels. Such mentioned proxies were in the models for explaining OP_v^{DTT} mostly combined with an organic wood burning emission tracer and for $PM_{2.5}$ also with copper and tin.

An alternative or supplementary interpretation of the above observations is that atmospheric ageing of PM and the changes that such processes induce modify the OP character of PM. Indeed, the importance of secondary PM ageing for OP has been shown by other work (Antiñolo et al., 2015; Wong et al., 2019; Zhu et al., 2020). Future studies will need to be conducted to
410 further fully understand these processes, however. This analysis is limited by the PM sampling campaign and associated PMF models that were able to be produced in this analysis. Further understanding of secondary PM sources and OP would be very useful to fully understand OP dynamics across Switzerland.

The combinations of pairs of independent variables in suitable models for explaining OP_v in PM_{10} and $PM_{2.5}$ as shown in Figure 7 indicates that the OP_v^{AA} assay provided a response that was more specific to the chemical composition of PM than the OP_v^{DTT} assay. It is also noticeable that for both OP_v assays there are more pairwise combinations of independent
415 variables in the suitable models for $PM_{2.5}$ than for PM_{10} (for OP_v^{AA}: 74 vs. 111 and for OP_v^{DTT}: 74 vs. 106). The reason for this observation is currently unclear and further research will be required to fully elucidate these features.

4   Conclusions

An intensive PM and OP sampling campaign conducted across Switzerland between 2018 and 2019 demonstrated that OP_v was
420 variable in time and space. OP_v patterns followed the familiar pattern of atmospheric pollutants where urban locations were more polluted than their rural counterparts and wintertime saw enhanced OP_v. Although the differences between rural and urban locations were important for mass, the OP metrics constantly showed a greater difference indicating OP was more heterogeneous than PM mass across Switzerland. When comparing Switzerland's OP_v with 14 sites in France where data exists and were produced by the same sampling and laboratory procedures, Switzerland's OP_v was comparable to that observed in France, but
425 Bern-Bollwerk, a semi-canyonised urban-traffic sampling location had the highest mean OP_v^{AA} ($4.1\,\mathrm{nmol\,min^{-1}\,m^{-3}}$) contained in the dataset. The lack of current standardisation for OP measurement, quantification, and calibration is an issue that the air quality community should address and would allow for reliable comparisons among different locations and times in the future. The AA and DTT assays showed much more seasonal structure than the third DCFH assay which made the former approaches more useful for data analysis than the latter.
430 An analysis of Switzerland's PM_{10} and $PM_{2.5}$ sources identified by PMF models suggested that two major anthropogenic emission sources, namely road traffic and wood combustion were the most important drivers of OP_v in Switzerland. The importance of these two sources for OP has been reported elsewhere too (Simonetti et al., 2018). Contrasting this was the inorganic nitrate- and sulfate-rich sources which generally had low levels of intrinsic OP_m across Switzerland, as did the two biogenic sources (primary and secondary). This outlines the potential disconnect between total PM mass concentration and
435 OP_m which has been noted by others, for example, Daellenbach et al. (2020) and this observation may update the management priorities of PM sources with a focus on health impacts rather than total mass.

Further investigation into the components of PM using a random forest dimensionality reduction technique and multiple linear regression models demonstrated that a collection of metals associated with non-exhaust emissions such as copper, zinc, antimony, iron, tin, manganese, and cadmium as well as the specific wood combustion tracers of levoglucosan, mannosan, and
440 galactosan (or associated elements such as rubidium and potassium) were consistently important for the explanation of OP_v. The combination of a non-exhaust sourced metal and a biomass burning tracer provided very good models which could explain OP_v well when considering their training sets.

The results above point toward the need to control wood burning sourced PM and non-exhaust emissions to reduce the OP_v of Switzerland's atmospheres. Such conclusions are not out of step with current air quality management practices and priorities,
445 but reinforce the importance of these sources and their respective chemistry with respect to OP_v – potentially a health-relevant metric for PM. Therefore, a renewed focus on wood burning and non-exhaust emissions is encouraged to reduce the deleterious health effects of PM. Because non-exhaust emissions and wood burning emissions can be effectively controlled at a local level, it is likely that significant reductions of OP_v could be achieved without the need for regional and transboundary management collaboration.

450 The causality of the identified sources (and PM constituents) for driving OP_v could always be questioned because the biological mechanisms which result in pathology were not investigated in this observational study. However, the results are consistent with those found in the literature and give very clear suggestions on where to focus future efforts to identify the linkage between biological mechanisms and OP_v. It is also clear that the PM_{10} and $PM_{2.5}$ size fractions have different OP_v characteristics and the OP_v is not simply additive. Furthermore, considering the importance of non-exhaust emissions for the
455 coarse-mode, the importance of continued PM_{10} monitoring is outlined.
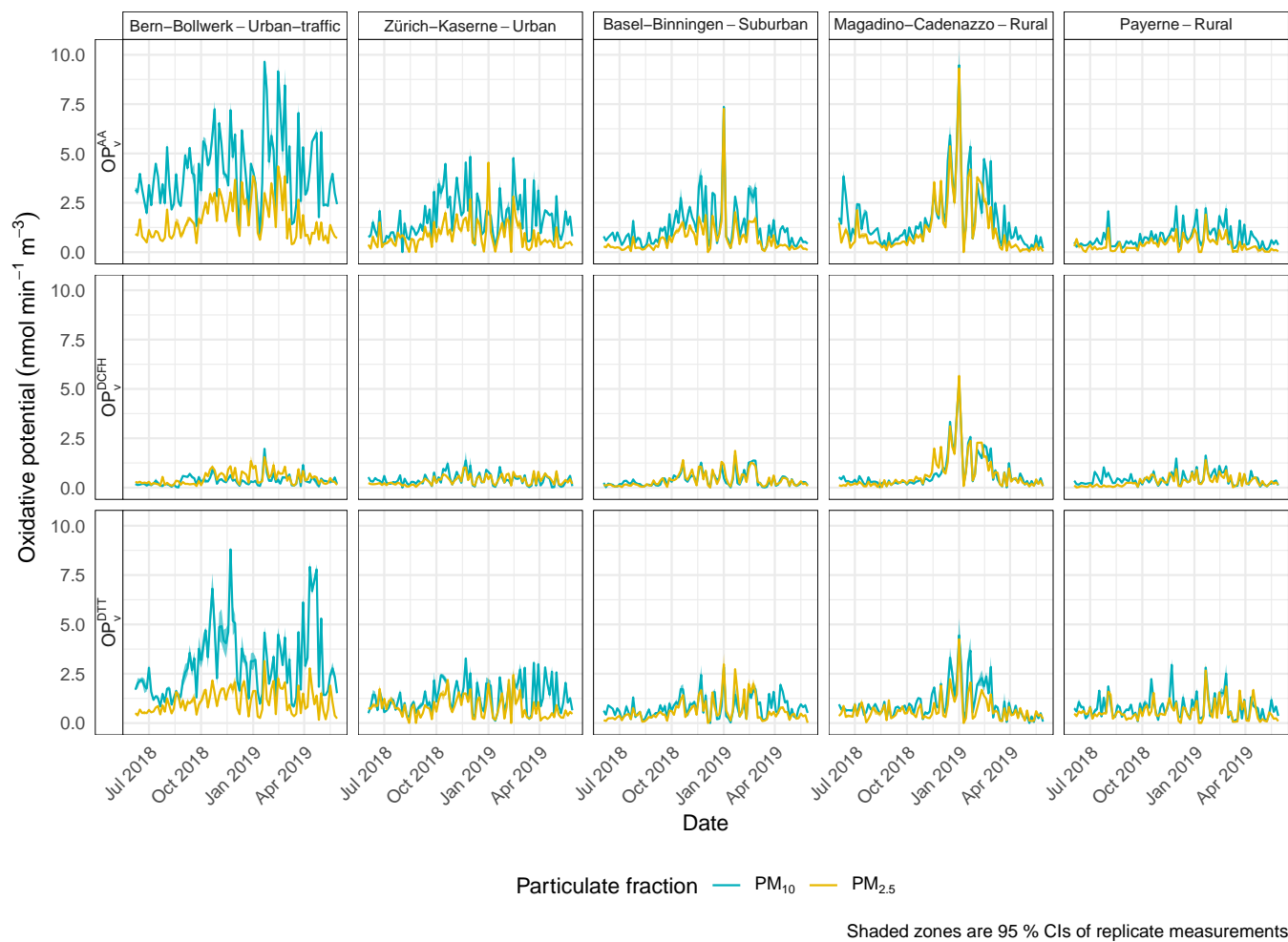
Figure A1. Time series of the three OP_v assays for PM_{10} and $PM_{2.5}$ at five sampling sites in Switzerland between June, 2018 and May, 2019.

Table A1. Annual means of PM_{10} OP_v^{AA} and OP_v^{DTT} for sampling sites in France and Switzerland where identical methods to quantify OP_v has been conducted. The units used for the means is $\mathrm{nmol\,min^{-1}\,m^{-3}}$ and the 14 sites' data from France are from Weber (2021); Weber et al. (2021).

Rank	Country	Urban area	Site	Site type	OP assay	Mean
1	Switzerland	Bern	Bern-Bollwerk	Traffic	OP_v^{AA}	4.1
2	France	Chamonix	CHAM	Urban valley	OP_v^{AA}	2.3
3	France	Nogent	NGT	Urban background	OP_v^{AA}	2.2
4	France	Passy	PAS	Urban valley	OP_v^{AA}	2.2
5	France	Roubaix	RBX	Traffic	OP_v^{AA}	2.1
6	Switzerland	Zürich	Zürich-Kaserne	Background	OP_v^{AA}	1.7
7	France	Aix-en-provence	AIX	Urban background	OP_v^{AA}	1.7
8	Switzerland	Cadenazzo	Magadino-Cadenazzo	Background	OP_v^{AA}	1.7
9	France	Grenoble	GRE-fr_2013	Urban background	OP_v^{AA}	1.7
10	France	Marnaz	MNZ	Urban valley	OP_v^{AA}	1.6
11	France	Vif	VIF	Urban background	OP_v^{AA}	1.5
12	France	Grenoble	GRE-fr_2017	Urban background	OP_v^{AA}	1.5
13	France	Grenoble	GRE-cb	Urban background	OP_v^{AA}	1.4
14	France	Strasbourg	STG-cle	Traffic	OP_v^{AA}	1.3
15	Switzerland	Basel	Basel-Binningen	Background	OP_v^{AA}	1.2
16	France	Talence	TAL	Urban background	OP_v^{AA}	1.0
17	France	Nice	NIC	Urban traffic	OP_v^{AA}	1.0
18	Switzerland	Payerne	Payerne	Background	OP_v^{AA}	0.7
19	France	Port-de-Bouc	PdB	Industrial	OP_v^{AA}	0.6
20	France	Marseille	MRS-5av	Urban background	OP_v^{AA}	0.5
1	France	Passy	PAS	Urban valley	OP_v^{DTT}	4.4
2	Switzerland	Bern	Bern-Bollwerk	Traffic	OP_v^{DTT}	2.9
3	France	Grenoble	GRE-fr_2013	Urban background	OP_v^{DTT}	2.7
4	France	Nogent	NGT	Urban background	OP_v^{DTT}	2.7
5	France	Roubaix	RBX	Traffic	OP_v^{DTT}	2.6
6	France	Marseille	MRS-5av	Urban background	OP_v^{DTT}	2.6
7	France	Strasbourg	STG-cle	Traffic	OP_v^{DTT}	2.4
8	France	Chamonix	CHAM	Urban valley	OP_v^{DTT}	2.3
9	France	Nice	NIC	Urban traffic	OP_v^{DTT}	2.2
10	France	Aix-en-provence	AIX	Urban background	OP_v^{DTT}	1.9
11	France	Talence	TAL	Urban background	OP_v^{DTT}	1.8
12	France	Marnaz	MNZ	Urban valley	OP_v^{DTT}	1.8
13	France	Port-de-Bouc	PdB	Industrial	OP_v^{DTT}	1.8
14	France	Grenoble	GRE-cb	Urban background	OP_v^{DTT}	1.7
15	France	Grenoble	GRE-fr_2017	Urban background	OP_v^{DTT}	1.5
16	Switzerland	Zürich	Zürich-Kaserne	Background	OP_v^{DTT}	1.3
17	France	Vif	VIF	Urban background	OP_v^{DTT}	1.3
18	Switzerland	Cadenazzo	Magadino-Cadenazzo	Background	OP_v^{DTT}	1.0
19	Switzerland	Payerne	Payerne	Background	OP_v^{DTT}	0.8
20	Switzerland	Basel	Basel-Binningen	Background	OP_v^{DTT}	0.8

Table A2. The number of multiple linear regression (MLR) models trained for each site, PM size fraction, and OP assay. The total number of models was 100 342.

Site	PM fraction	OP assay	Number of models trained
Basel-Binningen	PM_{10}	OP_{AA}	2379
Basel-Binningen	PM_{10}	OP_{DTT}	6884
Basel-Binningen	$PM_{2.5}$	OP_{AA}	4943
Basel-Binningen	$PM_{2.5}$	OP_{DTT}	6884
Bern-Bollwerk	PM_{10}	OP_{AA}	3472
Bern-Bollwerk	PM_{10}	OP_{DTT}	6884
Bern-Bollwerk	$PM_{2.5}$	OP_{AA}	4943
Bern-Bollwerk	$PM_{2.5}$	OP_{DTT}	6884
Magadino-Cadenazzo	PM_{10}	OP_{AA}	2379
Magadino-Cadenazzo	PM_{10}	OP_{DTT}	6884
Magadino-Cadenazzo	$PM_{2.5}$	OP_{AA}	4943
Magadino-Cadenazzo	$PM_{2.5}$	OP_{DTT}	6884
Payerne	PM_{10}	OP_{AA}	2379
Payerne	PM_{10}	OP_{DTT}	4943
Payerne	$PM_{2.5}$	OP_{AA}	3472
Payerne	$PM_{2.5}$	OP_{DTT}	4943
Zürich-Kaserne	PM_{10}	OP_{AA}	3472
Zürich-Kaserne	PM_{10}	OP_{DTT}	4943
Zürich-Kaserne	$PM_{2.5}$	OP_{AA}	4943
Zürich-Kaserne	$PM_{2.5}$	OP_{DTT}	6884

Table S1. Attached `op_model_collection_which_passed_the_filters.csv` file containing all linear regression model formulations with their estimates and model statistics.

Data availability. The data sources used in this work are described and some data sets are publicly accessible in a persistent data repository (Grange, 2021a, https://doi.org/10.5281/zenodo.4668158). Additional data and information are available from the authors on reasonable request.

Author contributions. SKG and CH conceived the research questions and wrote the manuscript. SKG conducted the data analysis and GU
460   managed the OP laboratory analyses. GU, SW, and JJ helped with revising and improving the manuscript.

Competing interests. The authors declare no competing interest.

Acknowledgements. This work was funded by the Federal Office for the Environment (FOEN) [contract number: 16.0096.PJ/R152-0739]. The authors thank the wider *Projekte Quellenzuordnung Feinstaub* team for their contributions. SKG is also supported by the Natural Environment Research Council (NERC) while holding associate status at the University of York. Andrés Alastuey and Xavier Querol from
465   Institute of Environmental Assessment and Water Research, Consejo Superior de Investigaciones Científicas are thanked for their help with the elemental ICP analysis. GU and JLJ thank the ANR-15-IDEX-02, ANR-19-CE34-0002-01, and Foundation of University of Grenoble Alpes for the funding of instruments on the AirOSol analytical plateau at IGE.

References

Abdulhammed, R., Musafer, H., Alessa, A., Faezipour, M., and Abuzneid, A.: Features Dimensionality Reduction Approaches for Machine Learning Based Network Intrusion Detection, Electronics, 8, https://doi.org/10.3390/electronics8030322, 2019.

Antiñolo, M., Willis, M. D., Zhou, S., and Abbatt, J. P. D.: Connecting the oxidation of soot to its redox cycling abilities, Nature Communications, 6, 6812, https://doi.org/10.1038/ncomms7812, 2015.

Barmpadimos, I., Hueglin, C., Keller, J., Henne, S., and Prévôt, A. S. H.: Influence of meteorology on PM_{10} trends and variability in Switzerland from 1991 to 2008, Atmospheric Chemistry and Physics, 11, 1813–1835, http://www.atmos-chem-phys.net/11/1813/2011/, 2011.

Bates, J., Fang, T., Verma, V., Zeng, L., Weber, R. J., Tolbert, P. E., Abrams, J. Y., Sarnat, S. E., Klein, M., Mulholland, J. A., and Russell, A. G.: Review of Acellular Assays of Ambient Particulate Matter Oxidative Potential: Methods and Relationships with Composition, Sources, and Health Effects, Environmental Science and Technology, 53, 4003–4019, https://doi.org/10.1021/acs.est.8b03430, 2019.

Behnamian, A., Banks, S., White, L., Millard, K., Pouliot, D., Pasher, J., and Duffe, J.: Dimensionality Reduction in The Presence of Highly Correlated Variables for Random Forests: Wetland Case Study, in: IGARSS 2019 - 2019 IEEE International Geoscience and Remote Sensing Symposium, pp. 9839–9842, https://doi.org/10.1109/IGARSS.2019.8898308, 2019.

Beyrich, F.: Mixing height estimation from sodar data – A critical discussion, Atmospheric Environment, 31, 3941 – 3953, https://doi.org/10.1016/S1352-2310(97)00231-8, 1997.

Borlaza, L. J. S., Cosep, E. M. R., Kim, S., Lee, K., Joo, H., Park, M., Bate, D., Cayetano, M. G., and Park, K.: Oxidative potential of fine ambient particles in various environments, Environmental Pollution, 243, 1679–1688, http://www.sciencedirect.com/science/article/pii/S0269749118332445, 2018.

Borlaza, L. J. S., Weber, S., Jaffrezo, J.-L., Houdier, S., Slama, R., Rieux, C., Albinet, A., Micallef, S., Trébluchon, C., and Uzu, G.: Disparities in particulate matter (PM_{10}) origins and oxidative potential at a city scale (Grenoble, France) – Part 2: Sources of PM_{10} oxidative potential using multiple linear regression analysis and the predictive applicability of multilayer perceptron neural network analysis, Atmospheric Chemistry and Physics, 21, 9719–9739, https://doi.org/10.5194/acp-21-9719-2021, 2021.

Breiman, L.: Random Forests, Machine Learning, 45, 5–32, https://doi.org/10.1023/A:1010933404324, 2001.

Bundesamt für Umwelt: Luftqualität 2020 – Messresultate des Nationalen Beobachtungsnetzes für Luftfremdstoffe (NABEL), https://www.bafu.admin.ch/dam/bafu/de/dokumente/luft/uz-umwelt-zustand/nabel-luftqualitaet-2020.pdf.download.pdf/UZ-2114-D_Jahrbuch_NABEL2020.pdf, Umwelt-Zustand Nr. 2114: 28 S, 2021.

Calas, A., Uzu, G., Martins, J. M. F., Voisin, D., Spadini, L., Lacroix, T., and Jaffrezo, J.-L.: The importance of simulated lung fluid (SLF) extractions for a more relevant evaluation of the oxidative potential of particulate matter, Scientific Reports, 7, 11 617, https://doi.org/10.1038/s41598-017-11979-3, 2017.

Calas, A., Uzu, G., Kelly, F. J., Houdier, S., Martins, J. M. F., Thomas, F., Molton, F., Charron, A., Dunster, C., Oliete, A., Jacob, V., Besombes, J.-L., Chevrier, F., and Jaffrezo, J.-L.: Comparison between five acellular oxidative potential measurement assays performed with detailed chemistry on PM_{10} samples from the city of Chamonix (France), Atmospheric Chemistry and Physics, 18, 7863–7875, https://doi.org/10.5194/acp-18-7863-2018, 2018.

Calas, A., Uzu, G., Besombes, J.-L., Martins, J. M. F., Redaelli, M., Weber, S., Charron, A., Albinet, A., Chevrier, F., Brulfert, G., Mesbah, B., Favez, O., and Jaffrezo, J.-L.: Seasonal Variations and Chemical Predictors of Oxidative Potential (OP) of Particulate Matter (PM), for Seven Urban French Sites, Atmosphere, 10, 698, https://www.mdpi.com/2073-4433/10/11/698, 2019.

505   Charrier, J. G. and Anastasio, C.: On dithiothreitol (DTT) as a measure of oxidative potential for ambient particles: evidence for the importance of soluble transition metals, Atmospheric Chemistry and Physics, 12, 9321–9333, https://doi.org/10.5194/acp-12-9321-2012, 2012.

Charron, A., Polo-Rehn, L., Besombes, J.-L., Golly, B., Buisson, C., Chanut, H., Marchand, N., Guillaud, G., and Jaffrezo, J.-L.: Identification and quantification of particulate tracers of exhaust and non-exhaust vehicle emissions, Atmospheric Chemistry and Physics, 19, 5187–

510   5207, https://doi.org/10.5194/acp-19-5187-2019, 2019.

Chen, G., Sosedova, Y., Canonaco, F., Fröhlich, R., Tobler, A., Vlachou, A., Daellenbach, K. R., Bozzetti, C., Hueglin, C., Graf, P., Baltensperger, U., Slowik, J. G., El Haddad, I., and Prévôt, A. S. H.: Time-dependent source apportionment of submicron organic aerosol for a rural site in an alpine valley using a rolling positive matrix factorisation (PMF) window, Atmospheric Chemistry and Physics, 21, 15 081–15 101, https://doi.org/10.5194/acp-21-15081-2021, 2021.

515   Cho, A. K., Sioutas, C., Miguel, A. H., Kumagai, Y., Schmitz, D. A., Singh, M., Eiguren-Fernandez, A., and Froines, J. R.: Redox Activity of Airborne Particulate Matter at Different Sites in the Los Angeles Basin, Environmental Research, 99, 40–47, https://doi.org/10.1016/j.envres.2005.01.003, 2005.

Daellenbach, K. R., Uzu, G., Jiang, J., Cassagnes, L.-E., Leni, Z., Vlachou, A., Stefenelli, G., Canonaco, F., Weber, S., Segers, A., Kuenen, J. J. P., Schaap, M., Favez, O., Albinet, A., Aksoyoglu, S., Dommen, J., Baltensperger, U., Geiser, M., El Haddad, I., Jaffrezo, J.-L.,

520   and Prévôt, A. S. H.: Sources of particulate-matter air pollution and its oxidative potential in Europe, Nature, 587, 414–419, https://doi.org/10.1038/s41586-020-2902-8, 2020.

Delfino, R. J., Staimer, N., Tjoa, T., Gillen, D. L., Schauer, J. J., and Shafer, M. M.: Airway inflammation and oxidative potential of air pollutant particles in a pediatric asthma panel, Journal of Exposure Science & Environmental Epidemiology, 23, 466–473, https://doi.org/10.1038/jes.2013.25, 2013.

525   Emeis, S. and Schäfer, K.: Remote Sensing Methods to Investigate Boundary-layer Structures relevant to Air Pollution in Cities, Boundary-Layer Meteorology, 121, 377–385, http://dx.doi.org/10.1007/s10546-006-9068-2, 2006.

European Committee for Standardization (CEN): CEN EN 16909: Ambient air – Measurement of elemental carbon (EC) and organic carbon (OC) collected on filters, Technical Committee: CEN/TC 264 – Air quality, 2017.

Fang, T., Verma, V., Bates, J. T., Abrams, J., Klein, M., Strickland, M. J., Sarnat, S. E., Chang, H. H., Mulholland, J. A., Tolbert, P. E., Russell,

530   A. G., and Weber, R. J.: Oxidative potential of ambient water-soluble $PM_{2.5}$ in the southeastern United States: contrasts in sources and health associations between ascorbic acid (AA) and dithiothreitol (DTT) assays, Atmospheric Chemistry and Physics, 16, 3865–3879, https://doi.org/10.5194/acp-16-3865-2016, 2016.

Fang, T., Zeng, L., Gao, D., Verma, V., Stefaniak, A. B., and Weber, R. J.: Ambient Size Distributions and Lung Deposition of Aerosol Dithiothreitol-Measured Oxidative Potential: Contrast between Soluble and Insoluble Particles, Environmental Science and Technology,

535   51, 6802–6811, https://doi.org/10.1021/acs.est.7b01536, 2017.

Favez, O., Salameh, D., and Jaffrezo, J.-L.: Traitement harmonisé de jeux de données multi-sites pour l'étude de sources de PM par Positive Matrix Factorization, https://bit.ly/2R3m1Cr, Laboratoire Central de Surveillance de la Qualité de l'Air. Ref. INERIS : DRC-16-152341-07444A, 2017.

Federal Office for the Environment: UNECE-CLRTAP Submission of air pollutant emissions for Switzerland 1980–2019, https://www.ceip.

540   at/status-of-reporting-and-review-results/2021-submission, deliveries for LRTAP Convention – National emission inventories. 12 Feb 2021 09:18, 2021.

Gao, D., Ripley, S., Weichenthal, S., and Godri Pollitt, K. J.: Ambient particulate matter oxidative potential: Chemical determinants, associated health effects, and strategies for risk management, Free Radical Biology and Medicine, 151, 7–25, https://doi.org/https://doi.org/10.1016/j.freeradbiomed.2020.04.028, air Pollution: Consequences for Cellular Redox Signaling, Antioxidant Defenses and Disease, 2020.

Gianini, M. F. D., Gehrig, R., Fischer, A., Ulrich, A., Wichser, A., and Hueglin, C.: Chemical composition of PM10 in Switzerland: An analysis for 2008/2009 and changes since 1998/1999, Atmospheric Environment, 54, 97–106, http://www.sciencedirect.com/science/article/pii/S1352231012001525, 2012.

Grange, S. K.: Data for publication "Switzerland's PM_{10} and $PM_{2.5}$ environmental increments show the importance of non-exhaust emissions", https://doi.org/10.5281/zenodo.4668158, 2021a.

Grange, S. K.: Example of training multiple linear regression (MLR) models to predict oxidative potential (OP) with other particulate matter (PM) constituents with simulated observations, https://gist.github.com/skgrange/1d5b2a51f478317bd0ccd9491eeb17c1, GitHub Gist, 2021b.

Grange, S. K.: Example of training multiple linear regression (MLR) models to explain/predict oxidative potential (OP) by particulate matter (PM) sources as identified by positive matrix factorisation (PMF) using simulated observations, https://gist.github.com/skgrange/60923587d3a39fc9dd440d053b3b7388, GitHub Gist, 2021c.

Grange, S. K., Carslaw, D. C., Lewis, A. C., Boleti, E., and Hueglin, C.: Random forest meteorological normalisation models for Swiss PM_{10} trend analysis, Atmospheric Chemistry and Physics, 18, 6223–6239, https://doi.org/https://doi.org/10.5194/acp-18-6223-2018, 2018.

Grange, S. K., Lötscher, H., Fischer, A., Emmenegger, L., and Hueglin, C.: Evaluation of equivalent black carbon source apportionment using observations from Switzerland between 2008 and 2018, Atmospheric Measurement Techniques, 13, 1867–1885, https://www.atmos-meas-tech.net/13/1867/2020/, 2020.

Grange, S. K., Fischer, A., Zellweger, C., Alastuey, A., Quero, X., Jaffrezo, J.-l., Weber, S., Uzu, G., and Hueglin, C.: Switzerland's PM_{10} and $PM_{2.5}$ environmental increments show the importance of non-exhaust emissions, Atmospheric Environment: X, 12, 100 145, https://doi.org/https://doi.org/10.1016/j.aeaoa.2021.100145, 2021.

Harrison, R. M.: Airborne particulate matter, Philosophical Transactions of the Royal Society A: Mathematical, Physical and Engineering Sciences, 378, 20190 319, https://doi.org/10.1098/rsta.2019.0319, 2020.

Harrison, R. M., Allan, J., Carruthers, D., Heal, M. R., Lewis, A. C., Marner, B., Murrells, T., and Williams, A.: Non-Exhaust Vehicle Emissions of Particulate Matter and VOC from Road Traffic: A Review, Atmospheric Environment, p. 118592, https://doi.org/https://doi.org/10.1016/j.atmosenv.2021.118592, 2021.

Hüglin, C. and Grange, S. K.: Chemical characterisation and source identification of PM_{10} and $PM_{2.5}$ in Switzerland, https://www.bafu.admin.ch/dam/bafu/de/dokumente/luft/externe-studien-berichte/chemical-characterisation-and-source-identification-of-pm-in-switzerland.pdf.download.pdf/Characterisation-source-identification-PM.pdf, Project report. Empa, Swiss Federal Laboratories for Materials Science and Technology. Commissioned by the Federal Office for the Environment (FOEN), 2021.

Jackson, L. S., Carslaw, N., Carslaw, D. C., and Emmerson, K. M.: Modelling trends in OH radical concentrations using generalized additive models, Atmospheric Chemistry and Physics, 9, 2021–2033, https://doi.org/10.5194/acp-9-2021-2009, 2009.

Janssen, N. A. H., Yang, A., Strak, M., Steenhof, M., Hellack, B., Gerlofs-Nijland, M. E., Kuhlbusch, T., Kelly, F., Harrison, R., Brunekreef, B., Hoek, G., and Cassee, F.: Oxidative potential of particulate matter collected at sites with different source characteristics, Science of The Total Environment, 472, 572–581, http://www.sciencedirect.com/science/article/pii/S0048969713014022, 2014.

580   Kelly, F. J. and Mudway, I. S.: Protein Oxidation at the Air-Lung Interface, Amino Acids, 25, 375–396, https://doi.org/10.1007/s00726-003-0024-x, 2003.

Kleeman, M. J., Schauer, J. J., and Cass, G. R.: Size and Composition Distribution of Fine Particulate Matter Emitted from Wood Burning, Meat Charbroiling, and Cigarettes, Environmental Science & Technology, 33, 3516–3523, https://doi.org/10.1021/es981277q, 1999.

Leni, Z., Cassagnes, L. E., Daellenbach, K. R., Haddad, I. E., Vlachou, A., Uzu, G., Prévôt, A. S. H., Jaffrezo, J.-L., Baumlin, N., Salathe, M.,
585   Baltensperger, U., Dommen, J., and Geiser, M.: Oxidative stress-induced inflammation in susceptible airways by anthropogenic aerosol, PLoS ONE, 15, e0233 425, https://doi.org/10.1371/journal.pone.0233425, 2020.

Liu, L., Urch, B., Szyszkowicz, M., Evans, G., Speck, M., Van Huang, A., Leingartner, K., Shutt, R. H., Pelletier, G., Gold, D. R., Brook, J. R., Godri Pollitt, K., and Silverman, F. S.: Metals and oxidative potential in urban particulate matter influence systemic inflammatory and neural biomarkers: A controlled exposure study, Environment International, 121, 1331–1340,
590   https://doi.org/https://doi.org/10.1016/j.envint.2018.10.055, 2018a.

Liu, W., Xu, Y., Liu, W., Liu, Q., Yu, S., Liu, Y., Wang, X., and Tao, S.: Oxidative potential of ambient $PM_{2.5}$ in the coastal cities of the Bohai Sea, northern China: Seasonal variation and source apportionment, Environmental Pollution, 236, 514–528, https://doi.org/10.1016/j.envpol.2018.01.116, 2018b.

Molina, C., Andrade, C., Manzano, C. A., Richard Toro, A., Verma, V., and Leiva-Guzmán, M. A.: Dithiothreitol-based oxidative potential for
595   airborne particulate matter: an estimation of the associated uncertainty, Environmental Science and Pollution Research, 27, 29 672–29 680, https://doi.org/10.1007/s11356-020-09508-3, 2020.

Norris, G., Duvall, R., Brown, S., and Bai, S.: EPA Positive Matrix Factorization (PMF) 5.0 Fundamentals and User Guide, https://www.epa.gov/air-research/epa-positive-matrix-factorization-50-fundamentals-and-user-guide, U.S. Environmental Protection Agency, EPA/600/R-14/108, April 2014, 2014.

600   Paatero, P.: The Multilinear Engine – A Table-Driven, Least Squares Program for Solving Multilinear Problems, Including the n-Way Parallel Factor Analysis Model, Journal of Computational and Graphical Statistics, 8, 854–888, https://doi.org/10.1080/10618600.1999.10474853, 1999.

Paatero, P. and Tapper, U.: Positive matrix factorization: A non-negative factor model with optimal utilization of error estimates of data values, Environmetrics, 5, 111–126, https://doi.org/10.1002/env.3170050203, 1994.

605   Perrone, M. G., Zhou, J., Malandrino, M., Sangiorgi, G., Rizzi, C., Ferrero, L., Dommen, J., and Bolzacchini, E.: PM chemical composition and oxidative potential of the soluble fraction of particles at two sites in the urban area of Milan, Northern Italy, Atmospheric Environment, 128, 104–113, https://doi.org/10.1016/j.atmosenv.2015.12.040, 2016.

Pietrogrande, M. C., Russo, M., and Zagatti, E.: Review of PM Oxidative Potential Measured with Acellular Assays in Urban and Rural Sites across Italy, Atmosphere, 10, https://doi.org/10.3390/atmos10100626, 2019.

610   Raaschou-Nielsen, O., Beelen, R., Wang, M., Hoek, G., Andersen, Z., Hoffmann, B., Stafoggia, M., Samoli, E., Weinmayr, G., Dimakopoulou, K., Nieuwenhuijsen, M., Xun, W., Fischer, P., Eriksen, K., Sørensen, M., Tjønneland, A., Ricceri, F., de Hoogh, K., Key, T., Eeftens, M., Peeters, P., de Mesquita, H. B., Meliefste, K., Oftedal, B., Schwarze, P., Nafstad, P., Galassi, C., Migliore, E., Ranzi, A., Cesaroni, G., Badaloni, C., Forastiere, F., Penell, J., De Faire, U., Korek, M., Pedersen, N., Östenson, C.-G., Pershagen, G., Fratiglioni, L., Concin, H., Nagel, G., Jaensch, A., Ineichen, A., Naccarati, A., Katsoulis, M., Trichpoulou, A., Keuken, M., Jedynska, A., Kooter, I.,
615   Kukkonen, J., Brunekreef, B., Sokhi, R., Katsouyanni, K., and Vineis, P.: Particulate matter air pollution components and risk for lung cancer, Environment International, 87, 66–73, https://doi.org/https://doi.org/10.1016/j.envint.2015.11.007, 2016.

Rausch, J., Jaramillo-Vogel, D., Perseguers, S., Schnidrig, N., Grobéty, B., and Yajan, P.: Automated identification and quantification of tire wear particles (TWP) in airborne dust: SEM/EDX single particle analysis coupled to a machine learning classifier, Science of The Total Environment, 803, 149 832, https://doi.org/https://doi.org/10.1016/j.scitotenv.2021.149832, 2022.

620 Reddy, G. T., Reddy, M. P. K., Lakshmanna, K., Kaluri, R., Rajput, D. S., Srivastava, G., and Baker, T.: Analysis of Dimensionality Reduction Techniques on Big Data, IEEE Access, 8, 54 776–54 788, https://doi.org/10.1109/ACCESS.2020.2980942, 2020.

Reid, J. S., Koppmann, R., Eck, T. F., and Eleuterio, D. P.: A review of biomass burning emissions part II: intensive physical properties of biomass burning particles, Atmospheric Chemistry and Physics, 5, 799–825, https://acp.copernicus.org/articles/5/799/2005/, 2005.

Saffari, A., Daher, N., Shafer, M. M., Schauer, J. J., and Sioutas, C.: Global Perspective on the Oxidative Potential of Airborne Particulate

625 Matter: A Synthesis of Research Findings, Environmental Science and Technology, 48, 7576–7583, https://doi.org/10.1021/es500937x, 2014.

Samake, A., Uzu, G., Martins, J. M. F., Calas, A., Vince, E., Parat, S., and Jaffrezo, J. L.: The unexpected role of bioaerosols in the Oxidative Potential of PM, Scientific Reports, 7, 10 978, https://doi.org/10.1038/s41598-017-11178-0, 2017.

Samaké, A., Jaffrezo, J.-L., Favez, O., Weber, S., Jacob, V., Albinet, A., Riffault, V., Perdrix, E., Waked, A., Golly, B., Salameh, D., Chevrier,

630 F., Oliveira, D. M., Bonnaire, N., Besombes, J.-L., Martins, J. M. F., Conil, S., Guillaud, G., Mesbah, B., Rocq, B., Robic, P.-Y., Hulin, A., Le Meur, S., Descheemaecker, M., Chretien, E., Marchand, N., and Uzu, G.: Polyols and glucose particulate species as tracers of primary biogenic organic aerosols at 28 French sites, Atmospheric Chemistry and Physics, 19, 3357–3374, https://acp.copernicus.org/articles/19/3357/2019/, 2019.

Samaké, A., Bonin, A., Jaffrezo, J.-L., Taberlet, P., Weber, S., Uzu, G., Jacob, V., Conil, S., and Martins, J. M. F.: High levels of primary

635 biogenic organic aerosols are driven by only a few plant-associated microbial taxa, Atmospheric Chemistry and Physics, 20, 5609–5628, https://doi.org/10.5194/acp-20-5609-2020, 2020.

Sandradewi, J., Prévôt, A., Weingartner, E., Schmidhauser, R., Gysel, M., and Baltensperger, U.: A study of wood burning and traffic aerosols in an Alpine valley using a multi-wavelength Aethalometer, Atmospheric Environment, 42, 101 – 112, https://doi.org/10.1016/j.atmosenv.2007.09.034, 2008.

640 Sandradewi, J., Prévôt, A. S. H., Szidat, S., Perron, N., Alfarra, M. R., Lanz, V. A., Weingartner, E., and Baltensperger, U.: Using Aerosol Light Absorption Measurements for the Quantitative Determination of Wood Burning and Traffic Emission Contributions to Particulate Matter, Environmental Science and Technology, 42, 3316–3323, https://doi.org/10.1021/es702253m, 2008.

Shirmohammadi, F., Wang, D., Hasheminassab, S., Verma, V., Schauer, J. J., Shafer, M. M., and Sioutas, C.: Oxidative potential of on-road fine particulate matter ($PM_{2.5}$) measured on major freeways of Los Angeles, CA, and a 10-year comparison with earlier roadside studies,

645 Atmospheric Environment, 148, 102–114, https://doi.org/https://doi.org/10.1016/j.atmosenv.2016.10.042, 2017.

Simonetti, G., Conte, E., Perrino, C., and Canepari, S.: Oxidative potential of size-segregated PM in an urban and an industrial area of Italy, Atmospheric Environment, 187, 292–300, https://doi.org/https://doi.org/10.1016/j.atmosenv.2018.05.051, 2018.

Svane, M., Hagström, M., and Pettersson, J. B. C.: Online Measurements of Individual Alkali-Containing Particles Formed in Biomass and Coal Combustion: Demonstration of an Instrument Based on Surface Ionization Technique, Energy Fuels, 19, 411–417,

650 https://doi.org/10.1021/ef049925g, 2005.

Taghvaee, S., Sowlat, M. H., Diapouli, E., Manousakas, M. I., Vasilatou, V., Eleftheriadis, K., and Sioutas, C.: Source apportionment of the oxidative potential of fine ambient particulate matter ($PM_{2.5}$) in Athens, Greece, Science of The Total Environment, 653, 1407–1416, https://doi.org/https://doi.org/10.1016/j.scitotenv.2018.11.016, 2019.

United Nations Human Rights Council: 48/13. The human right to a clean, healthy and sustainable environment, https://undocs.org/A/HRC/RES/48/13, forty-eighth session. 13 September–11 October 2021. Agenda item 3. Resolution adopted by the Human Rights Councilon 8 October 2021. A/HRC/RES/48/13, 2021.

Urban, R. C., Lima-Souza, M., Caetano-Silva, L., Queiroz, M. E. C., Nogueira, R. F., Allen, A. G., Cardoso, A. A., Held, G., and Campos, M. L. A.: Use of levoglucosan, potassium, and water-soluble organic carbon to characterize the origins of biomass-burning aerosols, Atmospheric Environment, 61, 562–569, https://doi.org/https://doi.org/10.1016/j.atmosenv.2012.07.082, 2012.

Venables, W. N. and Ripley, B. D.: Modern Applied Statistics with S, Springer, New York, fourth edn., http://www.stats.ox.ac.uk/pub/MASS4, ISBN 0-387-95457-0, 2002.

Weber, S.: Source apportionment of the Oxidative Potential of aerosols, http://getopstandop.u-ga.fr/, A visualisation tool and supplementary information, 2021.

Weber, S., Uzu, G., Calas, A., Chevrier, F., Besombes, J.-L., Charron, A., Salameh, D., Ježek, I., Močnik, G., and Jaffrezo, J.-L.: An apportionment method for the oxidative potential of atmospheric particulate matter sources: application to a one-year study in Chamonix, France, Atmospheric Chemistry and Physics, 18, 9617–9629, https://www.atmos-chem-phys.net/18/9617/2018/, 2018.

Weber, S., Salameh, D., Albinet, A., Alleman, L. Y., Waked, A., Besombes, J.-L., Jacob, V., Guillaud, G., Meshbah, B., Rocq, B., Hulin, A., Chrétien, M. D.-S. E., Jaffrezo, J.-L., and Favez, O.: Comparison of PM_{10} Sources Profiles at 15 French Sites Using a Harmonized Constrained Positive Matrix Factorization Approach, Atmosphere, 10, 310, https://doi.org/https://doi.org/10.3390/atmos10060310, 2019.

Weber, S., Uzu, G., Favez, O., Borlaza, L. J., Calas, A., Salameh, D., Chevrier, F., Allard, J., Besombes, J.-L., Albinet, A., Pontet, S., Mesbah, B., Gille, G., Zhang, S., Pallares, C., Leoz-Garziandia, E., and Jaffrezo, J.-L.: Source apportionment of atmospheric PM_{10} Oxidative Potential: synthesis of 15 year-round urban datasets in France, Atmospheric Chemistry and Physics, 21, 11 353–11 378, https://doi.org/10.5194/acp-21-11353-2021, 2021.

Wong, J. P. S., Tsagkaraki, M., Tsiodra, I., Mihalopoulos, N., Violaki, K., Kanakidou, M., Sciare, J., Nenes, A., and Weber, R. J.: Effects of Atmospheric Processing on the Oxidative Potential of Biomass Burning Organic Aerosols, Environmental Science & Technology, 53, 6747–6756, https://doi.org/10.1021/acs.est.9b01034, 2019.

World Health Organization: WHO global air quality guidelines: particulate matter ($PM_{2.5}$ and PM_{10}), ozone, nitrogen dioxide, sulfur dioxide and carbon monoxide, World Health Organization, https://apps.who.int/iris/rest/bitstreams/1371692/retrieve, 2021.

Wright, M. N. and Ziegler, A.: **ranger**: A Fast Implementation of Random Forests for High Dimensional Data in C++ and R, Journal of Statistical Software, 77, 1–17, https://doi.org/10.18637/jss.v077.i01, 2017.

Wright, M. N., Ziegler, A., and König, I. R.: Do little interactions get lost in dark random forests?, BMC Bioinformatics, 17, 145, http://www.ncbi.nlm.nih.gov/pmc/articles/PMC4815164/, 2016.

Yadav, S. and Phuleria, H. C.: Oxidative Potential of Particulate Matter: A Prospective Measure to Assess PM Toxicity, pp. 333–356, Springer Singapore, Singapore, https://doi.org/10.1007/978-981-15-0540-9_16, 2020.

Yang, A., Hellack, B., Leseman, D., Brunekreef, B., Kuhlbusch, T. A., Cassee, F. R., Hoek, G., and Janssen, N. A.: Temporal and spatial variation of the metal-related oxidative potential of $PM_{2.5}$ and its relation to $PM_{2.5}$ mass and elemental composition, Atmospheric Environment, 102, 62–69, https://doi.org/https://doi.org/10.1016/j.atmosenv.2014.11.053, 2015.

Yu, H., Puthussery, J. V., Wang, Y., and Verma, V.: Spatiotemporal variability in the oxidative potential of ambient fine particulate matter in the Midwestern United States, Atmospheric Chemistry and Physics, 21, 16 363–16 386, https://doi.org/10.5194/acp-21-16363-2021, 2021.

Yue, Y., Chen, H., Setyan, A., Elser, M., Dietrich, M., Li, J., Zhang, T., Zhang, X., Zheng, Y., Wang, J., and Yao, M.: Size-Resolved Endotoxin and Oxidative Potential of Ambient Particles in Beijing and Zürich, Environmental Science and Technology, 52, 6816–6824, https://doi.org/10.1021/acs.est.8b01167, 2018.

Zhang, Z., Weichenthal, S., Kwong, J. C., Burnett, R. T., Hatzopoulou, M., Jerrett, M., van Donkelaar, A., Bai, L., Martin, R. V., Copes, R., Lu, H., Lakey, P., Shiraiwa, M., and Chen, H.: A Population-Based Cohort Study of Respiratory Disease and Long-Term Exposure to Iron and Copper in Fine Particulate Air Pollution and Their Combined Impact on Reactive Oxygen Species Generation in Human Lungs, Environmental Science & Technology, 55, 3807–3818, https://doi.org/10.1021/acs.est.0c05931, 2021.

Zhu, J., Shang, J., Chen, Y., Kuang, Y., and Zhu, T.: Reactive Oxygen Species-Related Inside-to-Outside Oxidation of Soot Particles Triggered by Visible-Light Irradiation: Physicochemical Property Changes and Oxidative Potential Enhancement, Environmental Science & Technology, 54, 8558–8567, https://doi.org/10.1021/acs.est.0c01150, 2020.